AD-A177 940 APPLICATION OF THE VISCOUS-INVISCID INTERACTION METHOD TO THE ANALYSIS OF AIRFOIL FLOWS AT LOW REYNOLDS NUMBERS(U) NAVAL POSTGRADUATE SCHOOL MONTEREY CA 1/1

UNCLASSIFIED S W PAIK DEC 86 F/G 20/4 NL

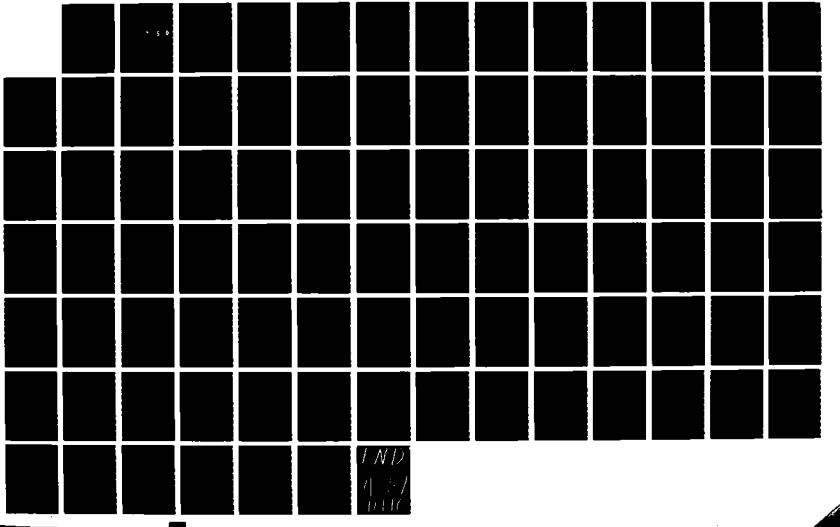

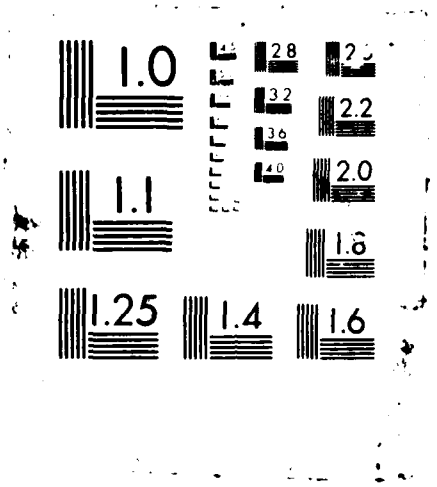
1.0
1.1
1.25
1.4
1.6
2.8
3.2
3.6
4.0
2.2
2.0
1.8

NAVAL POSTGRADUATE SCHOOL
Monterey, California

THESIS

APPLICATION OF THE VISCOUS-INVISCID INTERACTION METHOD TO THE ANALYSIS OF AIRFOIL FLOWS AT LOW REYNOLDS NUMBERS

by

Seung Woock Paik

December 1986

Thesis Advisor : M. F. Platzer

Approved for public release; distribution is unlimited

UNCLASSIFIED

SECURITY CLASSIFICATION OF THIS PAGE

REPORT DOCUMENTATION PAGE

1a REPORT SECURITY CLASSIFICATION Unclassified	1b RESTRICTIVE MARKINGS
2a SECURITY CLASSIFICATION AUTHORITY	3 DISTRIBUTION/AVAILABILITY OF REPORT Approved for public release ; distribution is unlimited
2b DECLASSIFICATION/DOWNGRADING SCHEDULE	
4 PERFORMING ORGANIZATION REPORT NUMBER(S)	5 MONITORING ORGANIZATION REPORT NUMBER(S)
6a NAME OF PERFORMING ORGANIZATION Naval Postgraduate School 6b OFFICE SYMBOL (If applicable) Code 67	7a NAME OF MONITORING ORGANIZATION Naval Postgraduate School
6c ADDRESS (City, State, and ZIP Code) Monterey, California 93943-5000	7b ADDRESS (City, State, and ZIP Code) Monterey, California 93943-5000
8a NAME OF FUNDING/SPONSORING ORGANIZATION 8b OFFICE SYMBOL (If applicable)	9 PROCUREMENT INSTRUMENT IDENTIFICATION NUMBER
8c ADDRESS (City, State, and ZIP Code)	10 SOURCE OF FUNDING NUMBERS PROGRAM ELEMENT NO / PROJECT NO / TASK NO / WORK UNIT ACCESSION NO

11 TITLE (Include Security Classification)
APPLICATION OF THE VISCOUS-INVISCID INTERACTION METHOD TO THE ANALYSIS OF AIRFOIL FLOWS AT LOW REYNOLDS NUMBERS

12 PERSONAL AUTHOR(S)
Paik, Seung W.

13a TYPE OF REPORT	13b TIME COVERED	14 DATE OF REPORT (Year Month Day)	15 PAGE COUNT
Master's Thesis	FROM _____ TO _____	1986, December	88

16 SUPPLEMENTARY NOTATION

17 COSATI CODES			18 SUBJECT TERMS (Continue on reverse if necessary and identify by block number)
FIELD	GROUP	SUB GROUP	viscous-inviscid interaction method airfoil flows

19 ABSTRACT (Continue on reverse if necessary and identify by block number)

The purpose of this thesis is to show the capability of strong Viscous/inviscid interaction methods to predict airfoil flows at low Reynolds numbers. Cebeci's interactive program was applied to the Wortmann-Althaus FX 63-137 airfoil and the results were compared with the available experimental data. It was found that the boundary layer transition model has an important influence on the predictive capability of viscous/inviscid interaction methods.

20 DISTRIBUTION/AVAILABILITY OF ABSTRACT	21 ABSTRACT SECURITY CLASSIFICATION
☒ UNCLASSIFIED/UNLIMITED ☐ SAME AS RPT ☐ DTIC USERS	Unclassified
22a NAME OF RESPONSIBLE INDIVIDUAL Prof. Max F. Platzer	22b TELEPHONE (Include Area Code) (408) 646-2944 22c OFFICE SYMBOL Code 67Pl

DD FORM 1473, 84 MAR 83 APR edition may be used until exhausted
All other editions are obsolete

SECURITY CLASSIFICATION OF THIS PAGE

UNCLASSIFIED

Approved for public release; distribution is unlimited.

Application of the Viscous-Inviscid Interaction Method to the Analysis of Airfoil Flows at Low Reynolds Numbers

by

Seung Woock, Paik
Captain, Republic of Korea Air Force
B.S.A.E., Korea Airforce Academy, Seoul, 1981

Submitted in partial fulfillment of the requirements for the degree of

MASTER OF SCIENCE IN AERONAUTICAL ENGINEERING

from the

NAVAL POSTGRADUATE SCHOOL
December 1986

Author: S. W. Paik
Seung Woock, Paik

Approved by: Max F. Platzer
Max F. Platzer, Thesis Advisor

Max F. Platzer
Max F. Platzer, Chairman,
Department of Aeronautics

John N. Dyer
John N. Dyer,
Dean of Science and Engineering

ABSTRACT

The purpose of this thesis is to show the capability of strong viscous/inviscid interaction methods to predict airfoil flows at low Reynolds numbers. Cebeci's interactive program was applied to the Wortmann-Althaus FX 63-137 airfoil and the results were compared with the available experimental data. It was found that the boundary layer transition model has an important influence on the predictive capability of viscous/inviscid interaction methods.

TABLE OF CONTENTS

LIST OF TABLES

LIST OF FIGURES

ACKNOWLEDGEMENTS

I make a grateful acknowledgement to Professor Platzer for his advice and stimulating my interest in the field of airfoil aerodynamics. I also give my thanks to Andreas Krainer for his assistance and to Dr. Cebeci for the use of his computer program.

I. INTRODUCTION

There are many theories to aid the airfoil design process by computational methods, because of the desire to reduce the number and cost of wind tunnel tests. A still largely unresolved question is the problem of flow separation. Because the classical boundary layer approximation cannot be applied to separated flow calculations, engineers have tried to overcome this limitation by developing viscous/inviscid interaction approaches or to develop direct solutions of the Navier-Stokes equation.

The purpose of this thesis is to demonstrate the capability of the viscous/inviscid interaction method by applying Cebeci's interactive computer program to a single airfoil (FX 63-137) at three low Reynolds numbers and by comparing the results with experimental data.

Chapter II explains the boundary layer theory. The boundary layer equations are derived and the turbulence models are introduced. Also, this chapter includes the prediction of transition boundary layer calculations and flow separation.

Chapter III introduces the interaction methods. Three weak interaction methods are explained briefly and the

simultaneous method is presented as a strong interaction method.

Chapter IV describes Cebeci's interactive computer program. Input/Output data description and JCL files are included. Also, the results of the application of Cebeci's program are discussed.

II. BOUNDARY LAYER THEORY

A. DERIVATION OF BOUNDARY LAYER EQUATIONS

Generally, the thickness of the boundary layer increases with viscosity, or it is possible to state that it decreases with viscosity, or it is possible to state that it decreases as the Reynolds number increases. From exact solutions of the Navier-Stokes equations, it was seen that the boundary-layer thickness (δ) is proportional to the square root of kinematic viscosity (ν);

$$\delta(x) \backsim \sqrt{\frac{\nu x}{U}}$$

where x is the distance from the leading edge of a flat plate. Using the local Reynolds number

$$Re = U\ x/\nu, \qquad \frac{\delta(x)}{x} \backsim \sqrt{\frac{1}{Re_x}}$$

For simplicity, assume a two-dimensional, steady constant - property flow without body forces and leave the stresses unspecified so that the results apply to laminar or turbulent flow. If simplifications are to be introduced into Navier-Stokes equations, it must be assumed that the boundary layer thickness is very small compared with a representative linear dimension (L) of the body, ie. $\delta \ll L$. In this way, the solutions obtained from the boundary layer

equations are asymptotic and apply to very large Reynolds numbers.

From the Navier-Stokes equations,

$$\text{x-direction: } -\frac{1}{\rho}\frac{\partial P}{\partial x} + \frac{1}{\rho}\frac{\partial \sigma_{xx}}{\partial x} + \frac{1}{\rho}\frac{\partial \sigma_{xy}}{\partial y} = u\frac{\partial u}{\partial x} + v\frac{\partial u}{\partial y}$$

$$\text{y-direction: } -\frac{1}{\rho}\frac{\partial P}{\partial y} + \frac{1}{\rho}\frac{\partial \sigma_{yy}}{\partial y} + \frac{1}{\rho}\frac{\partial \sigma_{xy}}{\partial x} = u\frac{\partial v}{\partial x} + v\frac{\partial v}{\partial y}$$

and the continuity equation is:

$$\frac{\partial u}{\partial x} + \frac{\partial v}{\partial y} = 0 \qquad (2.3)$$

Inserting the "typical" (order-of-magnitude) values, replace the dependent variables as follows;

$$u \backsim u_e\,, \quad \frac{\partial u}{\partial y} \backsim \frac{u_e}{\delta}\,, \quad \frac{\partial u}{\partial x} \backsim \frac{u_e}{l}$$

Then Eq. (2.1) can be expressed as

$$-\frac{1}{\rho}\frac{\partial P}{\partial x} + \frac{1}{\rho}\frac{\partial \sigma_{xx}}{\partial x} + \frac{1}{\rho}\frac{\partial \sigma_{xy}}{\partial y} = u\frac{\partial u}{\partial x} + v\frac{\partial u}{\partial y}$$

$$\frac{u_e^2}{l} \quad \frac{\sigma_{xx}/\rho}{l} \quad \frac{\sigma_{xy}/\rho}{l} \quad \frac{u_e^2}{l} \quad \frac{u_e^2}{l} \qquad (2.4)$$

where the typical values were written below the terms to which they correspond.

Considering turbulent flow, all stresses are of the same order ie. a general stress must be of order $\rho U_e^2 \delta/l$, then Eq. (2.1) becomes

$$-\frac{1}{\rho}\frac{\partial P}{\partial x} + \frac{1}{\rho}\frac{\partial \sigma_{xy}}{\partial y}\left[1 + O\left(\frac{\delta}{l}\right)\right] = u\frac{\partial u}{\partial x} + v\frac{\partial u}{\partial y} \qquad (2.5)$$

where $O(\delta/1)$ indicates a quantity of the order of magnitude of $\delta/1$.

Considering a laminar flow of Newtonian viscous fluid,

$$\sigma_{xx} = 2\mu \frac{\partial u}{\partial x}, \quad \sigma_{xy} = \mu\left(\frac{\partial u}{\partial y} + \frac{\partial v}{\partial x}\right), \quad \sigma_{yy} = 2\mu \frac{\partial v}{\partial y} \qquad (2.6)$$

In the σ_{xy} term, $\partial v/\partial x$ is smaller than $\partial u/\partial y$. Therefore, Eq. (2.5) becomes

$$-\frac{1}{\rho}\frac{\partial p}{\partial x} + \nu \frac{\partial^2 u}{\partial y^2}\left[1 + O\left(\frac{\delta}{1}\right)^2\right] = u\frac{\partial u}{\partial x} + v\frac{\partial u}{\partial y} \qquad (2.7)$$

Similarly, Eq. (2.2) can be written as:

$$-\frac{1}{\rho}\frac{\partial p}{\partial y} + \frac{1}{\rho}\frac{\partial \sigma_{yy}}{\partial y} + \frac{1}{\rho}\frac{\partial \sigma_{xy}}{\partial x} = u\frac{\partial v}{\partial x} + v\frac{\partial v}{\partial y}$$

$$\frac{1}{\rho}\frac{\partial p}{\partial y} \quad \frac{\nu u_e}{1\delta} \quad \nu\left(\frac{u_e}{1\delta}, \frac{u_e\delta}{1^3}\right) \quad \frac{u_e^2\delta}{1^2} \quad \frac{u_e^2\delta}{1^2} \qquad (2.8)$$

If we write all the viscous terms together,

$$\frac{1}{\rho}\frac{\partial p}{\partial y} \quad \frac{u_e^2\delta}{1^2} \quad \frac{\nu}{u_e 1}\left(\frac{1}{\delta}\right)^2\left[1, \left(\frac{\delta}{1}\right)^2\right] \quad \frac{u_e^2\delta}{1^2} \quad \frac{u_e^2\delta}{1^2} \qquad (2.9)$$

It is known that $(\delta/1)^2 \backsim \nu/u_e 1$ is laminar flow, so that the viscous terms are also of order $u_e^2\delta/1$ ie. $\partial P/\partial y$ is of order $u_e^2\delta/1^2$, but the pressure difference between $y=0$ and $y=\delta$ is of order $\rho u_e^2\delta^2/1^2$ and the difference in $\partial P/\partial x$ will be negligible compared to the external stream dynamic pressure, $1/2\,\rho u_e^2$. Therefore, for practical purposes,

$$\frac{\partial p}{\partial y} = 0 \qquad (2.10)$$

For this case, since changes in P must be of the same order as changes in y, the pressure does not change significantly through the boundary layer.

Thus, the entire equation of motion in the y-direction may be dropped from further considerations. In this way, the following simplified equations are left for the analysis of a boundary layer:

$$\frac{\partial u}{\partial x} + \frac{\partial v}{\partial y} = 0 \qquad (2.3)$$

$$-\frac{1}{\rho}\frac{\partial P}{\partial x} + \nu\frac{\partial^2 u}{\partial y^2} = u\frac{\partial u}{\partial x} + v\frac{\partial u}{\partial y} \qquad (2.11)$$

$$\frac{\partial P}{\partial y} = 0 \qquad (2.10)$$

These relations are known as Prandtl's boundary layer equations. Unless one encounters very high Mach numbers, the above orders of magnitude are not changed when compressibility effects are considered.

B. LAMINAR AND TURBULENT BOUNDARY LAYER

The low viscosity fluid flow past solid bodies should be considered as two regions. One is the thin region near the boundary in which the effects of viscosity are concentrated and the other is the region further away from the wall in which the influence of viscosity is so small that it can be neglected. Thus, it can be stated that all viscous effects are concentrated in the thin region which is known as the boundary layer. This boundary-layer type behavior requires

high Reynolds numbers. Generally, the thickness of the boundary layer (δ) is defined as that distance from the wall where the velocity (u) differs by 1% from that (Ue) calculated by the ideal flow analysis.

Consider a constant-property, steady, two-dimensional flow past a flat plate. If u/Ue is plotted against a dimensionless y-coordinate, $\eta = (Ue/\nu x)^{1/2} y$, the velocity profiles are geometrically similar and reduce to a single curve for a laminar boundary layer flow. This is well known as the Blasius profile. The geometrical similarity is maintained regardless of the Reynolds number of the flow or of the local skin friction. For a turbulent boundary layer flow, since the viscous-dependent part and the remaining Reynolds-stress-dependent part of the profile require different length scaling parameters, there is no choice of dimensionless y-coordinate that leads to the collapse of the complete set of velocity profiles into a single curve.

The conspicuous difference in profile shape between laminar and turbulent shear layers can be found in the wall flows. Because of the constraint on eddy size in wall flows, the efficiency of turbulent momentum transfer decreases rapidly near the wall. But, the efficiency of viscous momentum transfer is not dependent on y distance in the flow which has no heat transfer.

C. TURBULENCE MODELS

The unsteady continuity and Navier-Stokes Equations are valid in both laminar and turbulent flows. But, it is too difficult to deal with the instantaneous properties in turbulent flow because the turbulent flow has a complex time-dependent behavior. Thus, the following turbulence models are used to make the analysis of turbulent flow more convenient.

1. Prandtl's Mixing-Length

Consider two adjacent stream layers of fluid which move with different velocities. If a particle of fluid moves from one layer to the other, a momentum change occurs between two layers. The fast particles which enter the slow layer make it faster and the slow particles which enter the faster layer impose a drag on it.

The mean velocity of a stream layer is $\bar{u}$, and that of the other is $\bar{u} + l\ \partial \bar{u}/\partial y$ where l is the distance between two layers. Also, the fluctuating velocity in the x-direction is u', and that in the y-direction is v'. Prandtl assumed that the turbulent fluctuations are due to the difference in the mean velocities of the two layers. So $u' = l\ \partial \bar{u}/\partial y$ ie. the fluctuating velocity in the x-direction is of the order of the difference in the mean velocities of two layers which have a distance l, where l is the mixing length. Prandtl also assumed that all components of

fluctuating velocity at a given point are of the same order of magnitude. Thus, v' can be defined as $v' = k l \, \partial \bar{u}/\partial y$ where k is a constant.

The turbulent shear stress due to momentum exchange between two layers is the rate of momentum transfer per unit area. Then the mean turbulent shear stress on the fluid is $\tau_t = -\rho \overline{u'v'}$ where $\overline{u'v'} \propto |l \, \partial \bar{u}/\partial y| \; |k l \, \partial \bar{u}/\partial y|$. Since the values of l and k are unknown, combine these two unknowns. Then, $\tau_t = \rho l^2 |\partial \bar{u}/\partial y| \partial \bar{u}/\partial y$ where l is called the mixing length.

2. Cebeci-Smith Model

With the eddy viscosity concept, the momentum equation for 2-dimensional laminar and turbulent boundary layers can be written as:

$$(bf'')' + \frac{m+1}{2} ff'' + m\left[1 - (f')^2\right] = \bar{x}\left(f' \frac{\partial f'}{\partial \bar{x}} - f'' \frac{\partial f}{\partial \bar{x}}\right)$$

where $\bar{x}$ is the transformed x-variable

$$\bar{\varepsilon} = \varepsilon_m / \nu$$

$$b = (1 + t)^{2k} (1 + \bar{\varepsilon})$$

Let the turbulent boundary layer be a composite layer consisting of inner and outer regions. Then, the eddy-viscosity formula for the inner region is:

$$(\varepsilon_m)_i = l^2 \left(\frac{r}{r_0}\right)^k \left|\frac{\partial u}{\partial y}\right| \gamma_{tr} \qquad (0 \leq y \leq y_c)$$

where l is the mixing length for 2-dimensional flow

$$\gamma_{tr} = 1 - \exp\left[-\frac{1}{1200} R_{x_{tr}}^{0.66}\left(\frac{x}{x_{tr}} - 1\right)^2\right]$$

is an intermittency factor for a flat plate.

$R_{x_{tr}} = u_e x_{tr}/\nu$ is the transition Reynolds number.

The eddy-viscosity formula for the outer region is:

$$(\epsilon_m)_o = \alpha \left|\int_0^\infty (u_e - u)\, dy\right| \gamma_{tr} \quad (y \leq y \leq \delta)$$

where $R_\theta \geq 5000$, the universal constant $\alpha = 0.0168$.

$R_\theta < 5000$, α varies with R_θ according to the the empirical formula

$$\alpha = 0.0168 \quad \frac{1.55}{1 + \Lambda}$$

$$\Lambda = 0.55\left[1 - \exp\left(0.243\, h^{1/2} - 0.298\, h\right)\right]$$

$$h = R_\theta/425 - 1$$

But this model is not used in Cebeci's interactive computer program which will be presented in Chapter IV.

D. TRANSITION

The boundary layer with a finite thickness starts out as laminar at first in the flow past an airfoil. However, the boundary layer becomes unstable and all small disturbances begin transition to the erratically unsteady condition which is known as turbulence.

In the boundary layer on blunt bodies, transition makes the point of separation move downstream which decreases the width of the wake. There is an abrupt change in the drag curve of a sphere. This change is due to a boundary layer effect and is also one of the transition phenomena.

The process of transition on a flat plate at zero incidence shows a sudden increase in the boundary layer thickness. Furthermore, transition involves a great change in the shape of the velocity distribution and a large decrease in the ratio of the displacement thickness to the momentum thickness. Also, it causes a large change in the skin friction.

As described in the above, the transition from laminar to turbulent flow plays a very important role. Since the transition is not an instantaneous process and the flow is intermittently laminar and turbulent over a certain length of the airfoil, a certain point where transition takes place cannot be assigned. At present, there are no exact methods to calculate the flow within the transitional region. Nowadays, however, two methods - Michel's method and the e^9 method - are used to predict the transition empirically.

1. Michel's Method

Michel investigated many kinds of data for incompressible flows without heat transfer and found this empirical correlation,

$$R_\theta = 1.174 \left[1 + \frac{22400}{R_{x_{tr}}} \right] R_{x_{tr}}^{0.46}$$

where $R_\theta = Ue\ \theta/\nu$, $R_x = Ue\ x/\nu$.

Since the momentum thickness grows more rapidly when the pressure gradient is positive, Michel's equation involves the effect of pressure gradient. However, the

effect of surface roughness, which is also very important, is not included.

2. The e^9 Method

This e^9 method is of spatial amplification theory based on the solution of the Orr-Sommerfeld equation which forms the point of departure for the stability theory of laminar flows.

$$\left|\frac{g'}{g'}\right|_A = a = \exp \int_{x_A}^{x} \left(\alpha_i - \beta_i \frac{d\alpha_r}{d\beta_r}\right) dX$$

where $X = x/\delta^*$, $\alpha_i = \hat{\alpha}_i \delta^*$, $\beta_i = \hat{\beta}_i \delta^*$

$g'(x,y,z,t)$ is a typical disturbance function.

$\alpha = \frac{2\pi}{\lambda}$ (λ is the wavelength of the disturbance).

β_r is the circular frequency of the partial oscillation.

β_r is the amplification factor which determines the degree of amplification

The basic assumption is that transition begins at the point where a small disturbance introduced at the critical Reynolds number is amplified by a factor of e^9.

E. LAMINAR BOUNDARY LAYER CALCULATIONS

1. Similar Solutions

a. Blasius Solution For a Flat Plate

Assume - a flat plate at zero angle of attack

- steady, 2-D, laminar, incompressible flow.

- constant viscosity

- negligible body force

Since the pressure along the plate is constant, there is no pressure gradient. The simplified Navier-Stokes Equation is:

$$u \frac{\partial u}{\partial x} + v \frac{\partial u}{\partial y} = \nu \frac{\partial^2 u}{\partial y^2} \qquad (2.12)$$

(B,C) $y = 0;\ u = 0,\ v = 0$
$y = \infty;\ u = U_\infty$

To transform from the partial differential equation to an ordinary differential equation, define the following transformation parameter:

$$\eta = \sqrt{\frac{U_\infty}{\nu x}}\ y \qquad \text{where} \quad \eta = f(x,y)$$

$$\phi = \sqrt{\nu x U_\infty}\ f \qquad \text{where} \quad f = f(\eta) \text{ only}$$

The stream function was defined to satisfy the continuity equation.

$$u = \frac{\partial \phi}{\partial y} = \sqrt{\nu x U_\infty}\ \frac{df}{d\eta}\frac{\partial \eta}{\partial y} = U_\infty f', \text{ where } f' = \frac{df}{d\eta} \qquad (2.13)$$

$$\frac{\partial u}{\partial x} = U_\infty \frac{df'}{d\eta}\frac{\partial \eta}{\partial x} = U_\infty f'' y \sqrt{\frac{U_\infty}{\nu}} \left[-\frac{1}{2x^{3/2}} \right]$$

$$= -\frac{U_\infty f''}{2x}\eta \qquad (2.14)$$

$$v = -\frac{\partial \phi}{\partial x} = -\sqrt{\nu x U_\infty}\ \frac{df}{d\eta}\frac{\partial \eta}{\partial x} - \sqrt{\nu U_\infty}\ (1/2\ x^{-1/2})\ f$$

$$= 1/2\sqrt{\frac{\nu U_\infty}{x}}\ (f'\eta - f) \qquad (2.15)$$

$$\frac{\partial u}{\partial y} = U_\infty \frac{df'}{d\eta}\frac{\partial \eta}{\partial y} = U_\infty f''\sqrt{\frac{U_\infty}{\nu x}} \qquad (2.16)$$

$$\frac{\partial^2 u}{\partial y^2} = U_\infty \sqrt{\frac{U_\infty}{\nu x}} \frac{df''}{d\eta} \frac{\partial \eta}{\partial y} = \frac{U_\infty^2}{\nu x} f''' \qquad (2.17)$$

Substitute Eqs. (2.13) ~ (2.17) into Eq. (2.12), then

$$ff'' + 2f''' = 0$$

(B.C) $\eta = 0; \quad f' = 0, \quad f = 0$

$\eta = \infty; \quad f' = 1$

The solution of this Blasius equation is presented in "Boundary Layer Theory" by Schlichting. From the transformation relation,

$$\frac{\delta}{x} = \frac{5.0}{\sqrt{U_\infty x/\nu}} = \frac{5.0}{\sqrt{R_x}}, \qquad \frac{\delta^*}{x} = \frac{1.7208}{\sqrt{R_x}}$$

$$\left(\frac{v}{u}\right)_\infty = \frac{0.8604}{\sqrt{R_x}} \qquad \frac{\theta}{x} = \frac{0.664}{\sqrt{R_x}}$$

$$\tau_w = 0.332 \mu U_\infty \sqrt{\frac{V_\infty}{\nu x}}$$

$$C_f' = \frac{0.664}{\sqrt{R_x}}$$

b. Falkner-Skan Method

The Falkner-Skan transformation is for 2-D, axisymmetric laminar flow. The simplified Navier-Stokes Equation is:

$$u \frac{\partial u}{\partial x} + v \frac{\partial u}{\partial y} = -\frac{1}{\rho} \frac{\partial P}{\partial x} + \nu \frac{\partial^2 u}{\partial y^2}$$

(B.C) $y = 0; \quad u = 0, \quad v = 0$

$y = \infty; \quad u = U(x)$

Take the same η as Blasius' but different with a function $f = f(x, \eta)$ and follow the same procedure as Blasius' using

$-\frac{1}{\rho}\frac{dP}{dx} = U\frac{dU}{dx}$, then the transformed equation is:

$$f''' + \frac{m+1}{2} ff'' + m\left[1 - (f')^2\right] = x\left(f'\frac{\partial f'}{\partial x} - f''\frac{\partial f}{\partial x}\right)$$

where m is a dimensionless pressure gradient parameter defined by:

$$m = \frac{x}{U}\frac{dU}{dx}$$

(B.C) $\eta = 0$; $f' = 0$, $f = 0$

$\eta = \infty$; $f' = 1$

For similarity in 2-D, laminar flow, assume f is a function of η only. Then,

$$f''' + \frac{m+1}{2} ff'' + m\left[1 - (f')^2\right] = 0 \qquad (2.18)$$

(B.C) $\eta = 0$; f' = constant, $f' = 0$

$\eta = \infty$; $f' = 1$

The fact that m is a constant leads to:

$$U = c\,x^m$$

where c is also a constant.

In the case of m = 0, ie. U is a constant, Eq. (2.18) reduces to the Blasius equation. If m = 1 which means a 2-D stagnation flow, Eq. (2.18) becomes the Hiemenz equation,

$$f''' + ff'' - (f')^2 + 1 = 0$$

Some solutions of the Falkner-Skan equation for various values of m are presented by Cebeci and Bradshaw.

2. Integral Methods

a. Integral Momentum Equation

For steady, 2-D and incompressible flow,

$$u \frac{\partial u}{\partial x} + v \frac{\partial u}{\partial y} = -\frac{1}{\rho} \frac{\partial p}{\partial x} + \nu \frac{\partial^2 u}{\partial y^2} \qquad (2.19)$$

$$\frac{\partial u}{\partial x} + \frac{\partial v}{\partial y} = 0 \qquad (2.20)$$

From Eq. (2.20), $u \left(\frac{\partial u}{\partial x} + \frac{\partial v}{\partial y} \right) = 0$

At the edge of the boundary layer, $U(x) \frac{\partial U(x)}{\partial x} = -\frac{1}{\rho} \frac{\partial p}{\partial x}$

Then, Eq. (2.19) becomes:

$$\frac{\partial u^2}{\partial x} + \frac{\partial (uv)}{\partial y} = U(x) \frac{d U(x)}{dx} + \nu \frac{\partial^2 u}{\partial y^2}$$

Integrate this equation with respect to y, from y = 0 to $y = \delta$, using $\tau = \mu \frac{\partial u}{\partial y}$

$$\int_0^\delta \frac{\partial u^2}{\partial x} dy - \int_0^\delta U(x) \frac{\partial u}{\partial x} dy - \int_0^\delta U(x) \frac{dU(x)}{dx} dy = -\frac{\tau_w}{\rho} \qquad (2.21)$$

Also we know, $\delta^* = \int_0^\delta \left(1 - \frac{u}{U(x)}\right) dy$

$$\theta = \int_0^\delta \frac{u}{U(x)} \left(1 - \frac{u}{U(x)}\right) dy \qquad (2.22)$$

Substitute Eq. (2.22) into Eq. (2.21), then,

$$\frac{dU^2(x)\theta}{dx} + \delta^* U(x) \frac{dU(x)}{dx} = \frac{\tau_w}{\rho}$$

This equation is known as the momentum-integral equation of boundary layer theory, or as von Kármán's integral equation.

b. Pohlhausen's Method

Assume a polynomial of the fourth degree for the velocity function,

$$\frac{u}{U(x)} = f(\lambda) = a\lambda + b\lambda^2 + c\lambda^3 + d\lambda^4$$

where λ is the dimensionless distance from the wall,

$$\lambda = y/\delta \quad \text{and} \quad 0 < \lambda < 1$$

(B.C) $\lambda = 0;\quad f = 0,$

$\lambda = 1;\quad f = 1,\ f' = 0,\quad f'' = 0$

Also $U(x)\dfrac{d\,U(x)}{dx} + \nu\dfrac{\partial^2 u}{\partial y^2} = 0$ when $\lambda = 0$

$$\frac{\delta^2}{\nu}\frac{d\,U(x)}{dx} = -2b = \Lambda$$

where Λ is the shape factor.

then, $f(\lambda) = F(\lambda) + \Lambda G(\lambda)$

where $F(\lambda) = 2\lambda - 2\lambda^3 + \lambda^4$
$G(\lambda) = 1/6\,\lambda\,(1-\lambda)^3$

Thus the boundary layer parameters δ^*, θ and τ_w can be determined, if the velocity profile is known, as follows:

$$\frac{\delta^*}{\delta} = \frac{3}{10} - \frac{\Lambda}{120}$$

$$\frac{\theta}{\delta} = \frac{1}{63}\left(\frac{37}{5} - \frac{\Lambda}{15} - \frac{\Lambda^2}{144}\right)$$

$$\tau_w = \mu\frac{U(x)}{\delta}\left(2 + \frac{\Lambda}{6}\right)$$

c. Thwaites' Method

The integral momentum equation can be written as:

$$\frac{d\theta}{dx} + \frac{\theta}{U(x)}(H+2)\frac{dU(x)}{dx} = \frac{C_f}{2} \qquad (2.23)$$

(B.C) $y = 0;\ \dfrac{\partial^2 u}{\partial y^2} = -\dfrac{U(x)}{\theta^2}K,\ \dfrac{\partial u}{\partial y} = \dfrac{U(x)}{\theta}\quad L(K)$

where $H = \frac{\delta^*}{\theta}$

$$\frac{C_f}{2} = \frac{\tau_w}{\rho U^2(x)} = \frac{\nu L}{\theta U(x)}$$

$$K = \frac{\theta^2}{\nu} \frac{dU(x)}{dx}$$

then Eq. (2.23) can be reduced again.

$$\frac{U(x)}{\nu} \frac{d\theta^2}{dx} = 2 \left\{ L(K) - \left[H(K) + 2 \right] \right\} = F(K) \qquad (2.24)$$

Thwaites writes an expression for F(K)

$$F(K) = 0.45 - 6K$$

Then we can write Eq. (2.24) as

$$\frac{U(x)\theta^2}{\nu} = \frac{0.45}{U^5(x)} \int_0^x U^5(x)\, dx$$

If θ is calculated for a given external-velocity distribution, H and C_f can be determined with the following relations.

For $0 \leq K \leq 0.1$

$$L = 0.22 + 1.57K - 1.8K$$

$$H = 2.61 - 3.75K - 5.24K$$

For $-0.1 \leq K \leq 0$

$$L = 0.22 + 1.402K + \frac{0.018K}{0.107 + K}$$

$$H = \frac{0.0731}{0.14 + K} + 2.088$$

3. Finite-Difference Methods

The finite difference methods are the most flexible, practical and efficient methods to solve the boundary layer equations.

The box method, presented by Keller and Cebeci, is introduced here as the preferred finite-difference method. The momentum equation achieved by the Falkner-Skan transformation can be rewritten in terms of a first-order system of PDE's. Then the resulting non-linear system is linearized by Newton's method. Finally, the block elimination method is used to solve the linearized difference equations of the boundary layer problem.

a. Box Method.

Using the new coordinate system, ξ and η, the transformed momentum equation for steady, 2-D, incompressible flow becomes:

$$f' = u \tag{2.25a}$$

$$u' = v \tag{2.25b}$$

$$(bv)' + \frac{m+1}{2} fv + m(1-u^2) = \xi\left(u \frac{\partial u}{\partial \xi} - v \frac{\partial f}{\partial \xi}\right) \tag{2.25c}$$

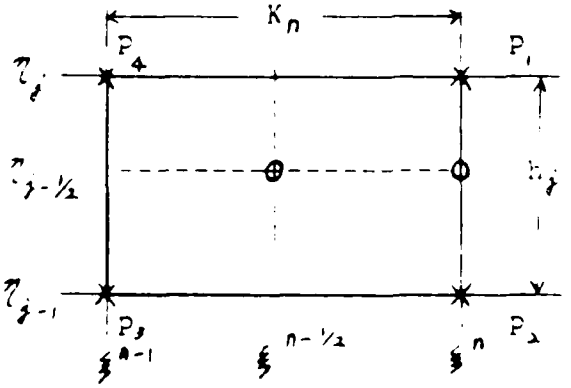

Figure 2.1 Net Rectangle For Difference Approximation

where $\xi = x$ and $b = 1 + \nu_t / \nu$

A prime denotes differentiation with respect to η.

The boundary conditions are

$$\eta = 0; \quad f(\xi, 0) = 0, \quad u(\xi, 0) = 0 \qquad (2.26)$$
$$\eta = \eta_\infty; \quad u(\xi, \eta_\infty) = 1$$

We denote the net points shown in Figure 2.1 by

$$\xi_0 = 0; \quad \xi^n = \xi^{n-1} + K_n \quad n = 1, 2, \ldots, n$$
$$\eta_0 = 0; \quad \eta_j = \eta_{j-1} + h_j \quad j = 1, 2, \ldots, J \qquad (2.27)$$
$$\eta_J = \eta_\infty$$

Here n and j indicate sequence numbers.

With $g_j^n = g(\xi n, \eta j)$ denoting the value of any quantity at the mesh point $(\xi n, \eta j)$, centered quantities can be written as two-point averages:

$$\xi^{n-1/2} = 1/2(\xi^n + \xi^{n-1}), \quad \eta_{j-1/2} = 1/2(\eta_j + \eta_{j-1}) \qquad (2.28a)$$
$$g_j^{n-1/2} = 1/2(g_j^n + g_j^{n-1}), \quad g_{j-1/2}^n = 1/2(g_j^n + g_{j-1}^n) \qquad (2.28b)$$

The finite difference approximations of Eqs. (2.25a) and (2.25b) for the mid point of the segment P_1, P_2 are:

$$\frac{f_j^n - f_{j-1}^n}{h_j} = u_{j-1/2}^n \qquad (2.29a)$$

$$\frac{u_j^n - u_{j-1}^n}{h_j} = v_{j-1/2}^n \qquad (2.29b)$$

Eq. (2.25c) can be approximated similarly by centering about the mid point of the rectangle P1,P2,P3,P4.

1. Centering Eq. (2.25c) about the point $(\xi^{n-1/2}, \eta)$

Let the left-hand side of Eq. (2.25c) be L and use Eq. (2.28b)

$$1/2\,(L^{n} + L^{n-1}) = \xi^{n-1/2}\left[U^{n-1/2}\left(\frac{u^{n} - u^{n-1}}{k_n}\right) - v^{n-1/2}\left(\frac{f^{n} - f^{n-1}}{k_n}\right)\right]$$

$$= \frac{\xi^{n-1/2}}{2K_n}\left[(u^2)^{n} - (u^2)^{n-1} - (fv)^{n} + f^{n-1}v^{n} - v^{n-1}f^{n} + (fv)^{n-1}\right]$$

By rearranging,

$$(bv')^{n} + \frac{m+1}{2}(fv)^{n} + m^{n}\left[1 - (u^2)^{n}\right]$$

$$= -L^{n-1} + \frac{\xi^{n-1/2}}{k_n}\left[(u^2)^{n} - (u^2)^{n-1} - (fv)^{n} + f^{n-1}v^{n} - v^{n-1}f^{n} + (fv)^{n-1}\right]$$

$$(bv')^{n} + \alpha_1(fv)^{n} - \alpha_2(u^2)^{n} + \alpha(v^{n-1}f^{n} - f^{n-1}v^{n}) = R^{n-1} \qquad (2.30)$$

where $\alpha = \dfrac{\xi^{n-1/2}}{K_n}$, $\alpha_1 = \dfrac{m^{n}+1}{2} + \alpha$, $\alpha_2 = m^{n} + \alpha$

$$R^{n-1} = -L^{n-1} + \alpha\left[(fv)^{n-1} - (u^2)^{n-1}\right] - m^{n}$$

$$L^{n-1} = \left[(bv)' + \frac{m+1}{2}(fv) + m(1-u^2)\right]^{n-1}$$

2. Centering Eq. (2.30) about the point $(\xi^{n-1/2}, \eta_{j-1/2})$ Using Eq. (2.29),

$$\left[(bv)'\right]^{n}_{j-1/2} = \frac{b^{n}_{j}v^{n}_{j} - b^{n}_{j-1}v^{n}_{j-1}}{h_j}$$

The Eq. (2.30) becomes

$$h_j^{-1}(b^{n}_{j}v^{n}_{j} - b^{n}_{j-1}v^{n}_{j-1}) + \alpha_1(fv)^{n}_{j-1/2} - \alpha_2(u^2)^{n}_{j-1/2}$$
$$+ \alpha(v^{n-1}_{j-1/2}f^{n}_{j-1/2} - f^{n-1}_{j-1/2}v^{n}_{j-1/2}) = R^{n-1}_{j-1/2} \qquad (2.31)$$

where

$$R^{n-1}_{j-1/2} = \left[-L_{j-1/2} + \alpha(fv)_{j-1/2} - (u^2)_{j-1/2}\right]^{n-1} - m^{n}$$

$$L^{n-1}_{j-1/2} = \left[h_j^{-1}(b_j v_j - b_{j-1}v_{j-1}) + \frac{m+1}{2}(fv)_{j-1/2} + m(1-u^2)_{j-1/2}\right]^{n-1}$$

The boundary conditions at $\xi = \xi^{n}$, are

$$f^{n}_{o} = 0, \qquad u^{n}_{o} = 0$$

$$u^{n}_{j} = 1, \qquad (2.32)$$

b. Newton's Method

For simplicity, let (f_j^n, u_j^n, v_j^n) be (f_j, u_j, v_j) at $\eta = \eta^n$.

Then Eq. (2.29) and 2.31) can be written as

$$f_j - f_{j-1} - \frac{h_j}{2}(u_j + u_{j-1}) = 0 \qquad (2.33a)$$

$$u_j - u_{j-1} - \frac{h_j}{2}(v_j + v_{j-1}) = 0 \qquad (2.33b)$$

$$h_j^{-1}(b_j v_j - b_{j-1} v_{j-1}) + \alpha_1 (fv)_{j-1/2} - \alpha_2 (u^2)_{j-1/2} + \alpha (v_{j-1/2}^{n-1} f_{j-1/2} - f_{j-1/2}^{n-1} v_{j-1/2}) = R_{j-1/2}^{n-1} \qquad (2.33c)$$

Here the unknowns are on the left-hand side and $R_{j-1/2}^{n-1}$ involves only known quantities.

Now, Newton's Method is applied to turn Eq.(2.33) into a linear system complemented by boundary conditions Eq.(2.32) and initial values

$$f_0^{(0)} = 0 \qquad u_0^{(0)} = 0 \qquad v_0^{(0)} = v_0^{n-1}$$

$$f_j^{(0)} = f_j^{n-1} \qquad u_j^{(0)} = u_j^{n-1} \qquad v_j^{(0)} = v_j^{n-1} \qquad (1 < j < J-1)$$

$$f_J^{(0)} = f_J^{n-1} \qquad u_J^{(0)} = 1 \qquad v_{(J)}^{(0)} = v_J^{n-1}$$

The superscripts in parenthesis represent the iteration number as follows:

$$f_j^{(i)}, \quad u_j^{(i)}, \quad v_j^{(i)} \qquad i = 0, 1, 2, \ldots$$

$$f_j^{(i+1)} = f_j^{(i)} + \delta f_j^{(i)}, \quad u_j^{(i+1)} = u_j^{(i)} + \delta u_j^{(i)}, \quad v_j^{(i+1)} = v_j^{(i)} + \delta v_j^{(i)}$$

where $\delta f \ll f$, $\delta u \ll u$, $\delta v \ll v$.

Replace f_j, u_j, v_j in Eq. (2.33) with these expressions. Then Eq.(2.33a) becomes:

$$f_j^{(i)} + \delta f_j^{(i)} - f_{j-1}^{(i)} - \delta f_{j-1}^{(i)} - \frac{h_j}{2}\left[u_j^{(i)} + \delta u_j^{(i)} + u_{j-1}^{(i)} + \delta u_{j-1}^{(i)}\right] = 0$$

Thus,

$$\delta f_j - \delta f_{j-1} - \frac{h_j}{2}\left[\delta u_j + \delta u_{j-1}\right] = (r_1)_j \qquad (2.34a)$$

where $(r_1)_j = f^{(i)}_{j-1} - f^{(i)}_j + h_j u^{(i)}_{j-1/2}$

From Eq. (2.33b),

$$u^{(i)}_j + \delta u^{(i)}_j - u^{(i)}_{j-1} - \delta u^{(i)}_{j-1} - \frac{h_j}{2}\left[v^{(i)}_j + \delta v^{(i)}_j + v^{(i)}_{j-1} + \delta v^{(i)}_{j-1}\right] = 0$$

$$\delta u_j - \delta u_{j-1} - \frac{h_j}{2}\left[\delta v_j + \delta v_{j-1}\right] = (r_3)_{j-1} \qquad (2.34b)$$

where $(r_3)_{j-1} = u^{(i)}_{j-1} - u^{(i)}_j + h_j v^{(i)}_{j-1/2}$

From Eq. (2.33c)

$$h_j^{-1}\left(b^{(i)}_j \delta v^{(i)}_j - b^{(i)}_{j-1}\,\delta v^{(i)}_{j-1}\right) + \alpha_1 \delta (fv)^{(i)}_{j-1/2} - \alpha_2 \delta (u^2)^{(i)}_{j-1/2}$$
$$+ \alpha\left(v^{n-1}_{j-1/2}\,\delta f^{(i)}_{j-1/2} - f^{n-1}_{j-1/2}\,\delta v^{(i)}_{j-1/2}\right)$$
$$= R^{n-1}_{j-1/2} - \left[h_j^{-1}\left(b^{(i)}_j v^{(i)}_j - b^{(i)}_{j-1}\,v^{(i)}_{j-1}\right) + \alpha_1 (fv)^{(i)}_{j-1/2} - \alpha_2 (u^2)^{(i)}_{j-1/2}\right.$$
$$\left. + \alpha\left(v^{n-1}_{j-1/2} f^{(i)}_{j-1/2} - f^{n-1}_{j-1/2} v^{(i)}_{j-1/2}\right)\right]$$

here $\delta (fv)^{(i)}_{j-1/2} = 1/2\left[f^{(i)}_j \delta v^{(i)}_j + v^{(i)}_j \delta f^{(i)}_j + f^{(i)}_{j-1}\delta v^{(i)}_{j-1} + v^{(i)}_{j-1}\delta f^{(i)}_{j-1}\right]$

$$\delta (u^2)^{(i)}_{j-1/2} = u^{(i)}_j \delta u^{(i)}_j + u^{(i)}_{j-1}\delta u^{(i)}_{j-1}$$

$$\delta f^{(i)}_{j-1/2} = 1/2\left(\delta f^{(i)}_j + \delta f^{(i)}_{j-1}\right)$$

$$\delta v^{(i)}_{j-1/2} = 1/2\left(\delta v^{(i)}_j + \delta v^{(i)}_{j-1}\right)$$

then $(s_1)_j \delta v_j + (s_2)_j \delta v_{j-1} + (s_3)_j \delta f_j + (s_4)_j \delta f_{j-1} + (s_5)_j \delta u_j$
$+ (s_6)_j \delta u_{j-1} = (r_2)_j \qquad (2.34c)$

where $(r_2)_j = R^{n-1}_{j-1/2} - \left[h_j^{-1}\left(b^{(i)}_j v^{(i)}_j - b^{(i)}_{j-1}\,v^{(i)}_{j-1}\right) + \alpha_1 (fv)^{(i)}_{j-1/2}\right.$
$\left. - \alpha_2 (u^2)^{(i)}_{j-1/2} + \alpha\left(v^{n-1}_{j-1/2} f^{(i)}_{j-1/2} - f^{n-1}_{j-1/2} v^{(i)}_{j-1/2}\right)\right]$

$$(s_1)_j = h_j^{-1} b^{(i)}_j + \frac{\alpha_1}{2} f^{(i)}_j - \frac{\alpha}{2} f^{n-1}_{j-1/2}$$

$$(s_2)_j = -h_j^{-1} b^{(i)}_{j-1} + \frac{\alpha_1}{2} f^{(i)}_{j-1} - \frac{\alpha}{2} f^{n-1}_{j-1/2}$$

$$(s_3)_j = \frac{\alpha_1}{2} v^{(i)}_j + \frac{\alpha}{2} v^{n-1}_{j-1/2}$$

$$(s_4)_j = \frac{\alpha_1}{2} v_{j-1}^{(i)} + \frac{\alpha}{2} v_{j-1/2}^{n-1}$$

$$(s_5)_j = -\alpha_2 u_j^{(i)}$$

$$(s_6)_j = -\alpha_2 u_{j-1}^{(i)}$$

the boundary conditions are:

$$\delta f_0 = 0 \qquad \delta u_0 = 0 \qquad \delta u_J = 0 \tag{2.35}$$

c. Block Elimination Method

Eqs.(2.34) and (2.35) are the linearized difference equations of the momentum equation for external flows which has a block tridiagonal structure. We can solve these equations by means of the Block Elimination Method as discussed by Keller (1974).

Let us define the three-dimensional vectors, δ_j and r_j, to express the system in matrix-vector form,

$$\delta_j = \begin{bmatrix} \delta f_j \\ \delta u_j \\ \delta v_j \end{bmatrix} \qquad 0 \leq j \leq J$$

$$r_0 = \begin{bmatrix} 0 \\ 0 \\ (r_3)_0 \end{bmatrix} \qquad r_j = \begin{bmatrix} (r_1)_j \\ (r_2)_j \\ (r_3)_j \end{bmatrix} \quad 1 \leq j \leq J-1 \tag{2.36}$$

$$r_J = \begin{bmatrix} (r_1)_J \\ (r_2)_J \\ 0 \end{bmatrix} \qquad j = J$$

and the 3 x 3 matrices, A_j , B_j , C_j

$$A_0 = \begin{bmatrix} 1 & 0 & 0 \\ 0 & 1 & 0 \\ 0 & -1 & -h_1/2 \end{bmatrix} \qquad A_j = \begin{bmatrix} 1 & -h_j/2 & 0 \\ (S_3)_j & (S_5)_j & (S_1)_j \\ 0 & -1 & -h_{j+1}/2 \end{bmatrix}$$

$$1 \le j \le J-1$$

$$A_J = \begin{bmatrix} 1 & -h_J/2 & 0 \\ (S_3)_J & (S_5)_J & (S_1)_J \\ 0 & 1 & 0 \end{bmatrix} \qquad j = J$$

(2.37)

$$B_j = \begin{bmatrix} 1 & -h_j/2 & 0 \\ (S_4)_j & (S_6)_j & (S_2)_j \\ 0 & 0 & 0 \end{bmatrix} \qquad 1 \le j \le J$$

$$C_j = \begin{bmatrix} 0 & 0 & 0 \\ 0 & 0 & 0 \\ 0 & 1 & -h_{j+1}/2 \end{bmatrix} \qquad 0 \le j \le J-1$$

Then Eqs. (2.34) and (2.35) can be written as

$$\mathcal{B}\,\delta = R \qquad (2.38)$$

where

$$\beta = \begin{bmatrix} A_0 & C_0 & & & & & & \\ B_1 & A_1 & C_1 & & & & & \\ & & & \ddots & & & & \\ & & & B_j & A_j & C_j & & \\ & & & & & & \ddots & \\ & & & & & B_{J-1} & A_{J-1} & C_{J-1} \\ & & & & & & B_J & A_J \end{bmatrix} \quad \delta = \begin{bmatrix} \delta_0 \\ \delta_1 \\ \vdots \\ \delta_j \\ \vdots \\ \delta_{J-1} \\ \delta_J \end{bmatrix} \quad R = \begin{bmatrix} r_0 \\ r_1 \\ \vdots \\ r_j \\ \vdots \\ r_{J-1} \\ r_J \end{bmatrix}$$

Let us factorize the matrix β to solve Eq. (2.38)

$$\beta = xy \tag{2.39}$$

where

$$\beta = \begin{bmatrix} I & & & & & \\ x_1 & I & & & & \\ & & \ddots & & & \\ & & x_j & I & & \\ & & & & \ddots & \\ & & & & x_J & I \end{bmatrix} * \begin{bmatrix} y_0 & C_0 & & & & \\ & y_1 & C_1 & & & \\ & & & \ddots & & \\ & & & y_j & C_j & \\ & & & & & \ddots \\ & & & & & y_J \end{bmatrix}$$

Here I is the 3 x 3 identity matrix.

x_j and y_j are also 3 x 3 matrices.

According to Eq.(2.39), we can find

$$y_0 = A_0 \tag{2.40a}$$

$$x_j\, y_{j-1} = B_j \quad (j = 1,2,\ldots, J) \tag{2.40b}$$

$$y_j = A_j - x_j\, C_{j-1} \quad (j = 1,2\ldots, J) \tag{2.40c}$$

and the matrix x_j has the same structure as that of the matrix B_j. Therefore, x_j has the elements like this,

$$x_j = \begin{bmatrix} (x_{11})_j & (x_{12})_j & (x_{13})_j \\ (x_{21})_j & (x_{22})_j & (x_{23})_j \\ 0 & 0 & 0 \end{bmatrix}$$

and y_j can be denoted as:

$$y = \begin{bmatrix} (y_{11})_j & (y_{12})_j & (y_{13})_j \\ (y_{21})_j & (y_{22})_j & (y_{23})_j \\ 0 & -1 & -h_{j+1}/2 \end{bmatrix}$$

From Eq. (2.40a),

$$(y_{11})_0 = 1 \qquad (y_{12})_0 = 0 \qquad (y_{13})_0 = 0$$
$$(y_{21})_0 = 0 \qquad (y_{22})_0 = 1 \qquad (y_{23})_0 = 0$$

From Eq. (2.40b)

$$(x_{11})_1 = -1 \qquad (x_{12})_1 = -1/2\ h_1 \qquad (x_{13})_1 = 0$$
$$(x_{21})_1 = (s_4)_1 \qquad (x_{22})_1 = (s_6)_1 + (x_{23})_1 \qquad (x_{23})_1 = -2\ (s_2)_1/h_1$$

From Eq. (2.40c)

$$(y_{11})_j = 1 \qquad (y_{12})_j = -\frac{h_j}{2} - (x_{13})_j \qquad (y_{13})_j = \frac{h_j}{2}(x_{13})_j$$

$$(y_{21})_j = (s_3)_j \qquad (y_{22})_j = (s_5)_j - (x_{23})_j \qquad (y_{23})_j = (s_1)_j + \frac{h_{j+1}}{2}(x_{23})_j$$

Then we can compute the elements of x with Eqs. (2.37) and (2.40b) for $1 \le j \le J$,

$$(x_{11})_j = \frac{1}{y_0}\left\{(y_{23})_{j-1} + \frac{h_j}{2}\left[\frac{h_j}{2}(y_{21})_{j-1} - (y_{22})_{j-1}\right]\right\}$$

$$(x_{12})_j = -\frac{1}{y_1}\left\{\left(\frac{h_j}{2}\right)^2 + (x_{11})_j\left[(y_{12})_{j-1}\frac{h}{2} - (y_{13})_{j-1}\right]\right\}$$

$$(x_{13})_j = \frac{h_j}{2}\left[(x_{11})_j (y_{13})_{j-1} + (x_{12})_j (y_{23})_{j-1}\right]$$

$$(x_{21})_j = \frac{1}{y_0}\left\{(s_2)_j (y_{21})_{j-1} + (s_4)_j (y_{23})_{j-1} + \frac{h_j}{2}\left[(s_4)_j (y_{22})_{j-1} - (s_6)_j (y_{21})_{j-1}\right]\right\}$$

$$(x_{22})_j = \frac{1}{y_1}\left\{\frac{h_j}{2}(s_6)_j - (s_2)_j + (x_{21})_j\left[(y_{13})_{j-1} - \frac{h_j}{2}(y_{12})_{j-1}\right]\right\}$$

$$(x_{23})_j = (x_{21})_j (y_{12})_{j-1} + (x_{22})_j (y_{22})_{j-1} - (s_6)_j$$

$$y_0 = (y_{13})_{j-1}(y_{21})_{j-1} - (y_{23})_{j-1}(y_{11})_{j-1} - \frac{h_j}{2}\left[(y_{12})_{j-1}(y_{21})_{j-1} - (y_{22})_{j-1}(y_{11})_{j-1}\right]$$

$$y_1 = \frac{h_j}{2} (y_{22})_{j-1} - (y_{23})_{j-1}$$

Let $y\delta = z$, then $xz = R$ (2.41)

Thus, $z_0 = r_0$ (2.42)

$$z_j = r_0 - x_j z_{j-1} \qquad (1 \leq j \leq J)$$

where $$z_j = \begin{bmatrix} (z_1)_j \\ (z_2)_j \\ (z_3)_j \end{bmatrix} \qquad (0 \leq j \leq J)$$

From Eq. (2.42) for j = 0

$$(z_1)_0 = (r_1)_0 \qquad (z_2)_0 = (r_2)_0 \qquad (z_3)_0 = (r_3)_0$$

and for $1 \leq j \leq J$

$$(z_1)_j = (r_1)_j - (x_{11})_j (z_1)_{j-1} - (x_{12})_j (z_2)_{j-1} - (x_{13})_j (z_3)_{j-1}$$

$$(z_2)_j = (r_2)_j - (x_{21})_j (z_1)_{j-1} - (x_{22})_j (z_2)_{j-1} - (x_{23})_j (z_3)_{j-1}$$

$$(z_3)_j = (r_3)_j$$

From Eq. (2.41),

$$y_J \delta_J = z_J \qquad (2.43a)$$

$$y_j \delta_j = z_j - c_j \delta_{j+1} \qquad (0 \leq j \leq J-1) \qquad (2.43b)$$

Then the vectors can be calculated with Eq. (2.43). The three components of , for j = 0,1,2,...J-1, are:

$$\delta U_j = - \frac{h_{j+1}}{2} \delta v_j - e_1$$

$$\delta v_j = \frac{1}{y_2} \left\{ (y_{11})_j \left[(z_2)_j + e_1 (y_{22})_j \right] - (y_{21})_j (z_1)_j - e_1 (y_{21})_j (y_{12})_j \right\}$$

$$\delta w_j = \frac{1}{(y_{11})_j} \left[(z_1)_j - (y_{12})_j \delta u_j - (y_{13})_j \delta v_j \right]$$

where $e_1 = (z_3)_j - \delta u_{j+1} + \frac{h_{j+1}}{2} \delta v_{j+1}$

$$y_2 = \frac{h_{j+1}}{2}\left[(y_{21})_j (y_{12})_j + (y_{22})_j (y_{11})_j\right]$$

$$- (y_{21})_j (y_{13})_j + (y_{23})_j (y_{11})_j$$

and for j = J

$$\delta u_J = (z_3)_J$$

$$\delta v_J = \frac{e_2 (y_{21})_J - e_3 (y_{11})_J}{(y_{13})_J (y_{21})_J - (y_{23})_J (y_{11})_J}$$

$$\delta w_J = \frac{e_2 - (y_{13})_J \delta v_J}{(y_{11})_J}$$

where $e_2 = (z_1)_J - (y_{12})_J \delta u_J$

$e_3 = (z_2)_J - (y_{22})_J \delta u_J$

These calculations are stopped when

$$|\delta v_0^{(i)}| < \varepsilon$$

where v(o) is the wall shear parameter.

ε is a prescribed value.

F. TURBULENT BOUNDARY LAYER CALCULATIONS

Turbulent fluid motion is an irregular condition of flow in which the various quantities show a random variation with time and space. Therefore, turbulence is characterized by random and chaotic motion of fluid particles.

The velocity varies randomly at any point in a turbulent fluid. The velocity components in a three-dimensional turbulent fluid are:

$$u = \bar{u} + u'$$

$$v = \bar{v} + v'$$

$$w = \bar{w} + w'$$

where $\bar{u}$, $\bar{v}$, $\bar{w}$ represent the mean velocities

$$\bar{u} = \frac{1}{t_2 - t_1} \int_{t_1}^{t_2} u \, dt, \text{ and so on.}$$

u', v', w' represent the amount of fluctuation of the instantaneous velocities from the mean velocities.

Obviously, we can see that

$$\frac{1}{t_2 - t_1} \int_{t_1}^{t_2} u' \, dt = \overline{u'} = o, \text{ etc.}$$

Similarly, the following quantities can be defined,

$$\frac{1}{t_2 - t_1} \int_{t_1}^{t_2} u'^2 \, dt = \overline{u'^2}, \text{ etc.}$$

$$\frac{1}{t_2 - t_1} \int_{t_1}^{t_2} u'v' \, dt = \overline{u'v'}, \text{ etc.}$$

Even though the flow is turbulent, the time-dependent momentum equations are valid. However, it is impossible to solve the momentum equations for turbulent flow because the fluctuations are random and chaotic. Thus, Reynolds modified the momentum equations by introducing the mean value and fluctating values of the flow quantities and by assuming the fluctuations to be continuous functions of time and space. From the momentum equations,

$$\frac{\partial u}{\partial t} + u\frac{\partial u}{\partial x} + v\frac{\partial u}{\partial y} + w\frac{\partial u}{\partial z} = \frac{-1}{\rho}\frac{\partial p}{\partial x} + \nu\left(\frac{\partial^2 u}{\partial x^2} + \frac{\partial^2 u}{\partial y^2} + \frac{\partial^2 u}{\partial z^2}\right)$$

By multiplying the continuity equations with u

$$u\left(\frac{\partial u}{\partial x} + \frac{\partial v}{\partial y} + \frac{\partial w}{\partial z}\right) = 0$$

Sum these two equations and rearrange, then,

$$\frac{\partial u}{\partial t} = -\frac{1}{\rho}\frac{\partial p}{\partial x} + \frac{\partial}{\partial x}\left(\nu\frac{\partial u}{\partial x} - u^2\right) + \frac{\partial}{\partial y}\left(\nu\frac{\partial u}{\partial y} - uv\right) + \frac{\partial}{\partial z}\left(\nu\frac{\partial u}{\partial z} - uw\right)$$

Here take the mean value of each term using $\overline{u'} = 0$,

$$\frac{\partial\overline{(\bar{u} + u')}}{\partial t} = \frac{\partial\bar{\bar{u}}}{\partial t} + \frac{\partial\bar{u}'}{\partial t} = \frac{\partial\bar{u}}{\partial t}$$

$$-\frac{1}{\rho}\frac{\partial\overline{(\bar{P} + P')}}{\partial x} = \frac{-1}{\rho}\frac{\partial\bar{P}}{\partial x}$$

$$\nu\frac{\partial\overline{(\bar{u} + u')}}{\partial x} - \overline{(\bar{u} + u')^2} = \nu\frac{\partial\bar{u}}{\partial x} - (\bar{\bar{u}}^2 + \overline{2\,\bar{u}u'} + \overline{u'^2})$$

$$= \nu\frac{\partial\bar{u}}{x} - \bar{u}^2 - \overline{u'^2}$$

$$\nu\frac{\partial\overline{(\bar{u} + u')}}{\partial y} = \nu\frac{\partial\bar{u}}{\partial y} - \overline{uv} - \overline{u'v'}$$

$$\nu\frac{\partial\overline{(\bar{u} + u')}}{\partial z} = \nu\frac{\partial\bar{u}}{\partial z} - \overline{uw} - \overline{u'w'} \qquad (2.45)$$

Substitute Eq. (2.45) into Eq. (2.44) and rearrange. Then,

$$\rho\left(\frac{\partial\bar{u}}{\partial t} + \bar{u}\frac{\partial\bar{u}}{\partial x} + \bar{v}\frac{\partial\bar{u}}{\partial y} + \bar{w}\frac{\partial\bar{u}}{\partial z}\right)$$

$$= -\frac{\partial\bar{P}}{\partial x} + \mu\nabla^2\bar{u} - \rho\left(\frac{\partial\overline{u'^2}}{\partial x} + \frac{\partial\overline{u'v'}}{\partial y} + \frac{\partial\overline{u'w'}}{\partial z}\right) \qquad (2.46a)$$

By similar procedures for the other directions,

$$\rho\left(\frac{\partial\bar{v}}{\partial t} + \bar{u}\frac{\partial\bar{v}}{\partial x} + \bar{v}\frac{\partial\bar{v}}{\partial y} + \bar{w}\frac{\partial\bar{v}}{\partial z}\right)$$

$$= -\frac{\partial\bar{P}}{\partial y} + \mu\nabla^2\bar{v} - \rho\left(\frac{\partial\overline{v'u'}}{\partial x} + \frac{\partial\overline{v'^2}}{\partial y} + \frac{\partial\overline{v'w'}}{\partial z}\right) \qquad (2.46b)$$

$$\rho\left(\frac{\partial\bar{w}}{\partial t} + \bar{u}\frac{\partial\bar{w}}{\partial x} + \bar{v}\frac{\partial\bar{w}}{\partial y} + \bar{w}\frac{\partial\bar{w}}{\partial z}\right)$$

$$= -\frac{\partial\bar{P}}{\partial z} + \mu\nabla^2\bar{w} - \rho\left(\frac{\partial\overline{w'u'}}{\partial x} + \frac{\partial\overline{w'v'}}{\partial y} + \frac{\partial\overline{w'^2}}{\partial z}\right) \qquad (2.46c)$$

and from the continuity equation,

$$\frac{\partial\bar{u}}{\partial x} + \frac{\partial\bar{v}}{\partial y} + \frac{\partial\bar{w}}{\partial z} = 0 \qquad (2.47)$$

In laminar flow, we have 4 unknowns and 4 equations. But in turbulent flow, we have 10 unknowns and only 4 equations as shown at Eqs.(2.46), (2.47). This is the reason why we need the turbulence models which were discussed in Section C.

G. SEPARATION

In some cases, the boundary layer thickness increases considerably in the downstream direction and the flow in the boundary layer reverses its direction. The change in direction causes the decelerated fluid particles to move outwards, which means that the boundary layer is separated from the wall. This phenomenon, boundary layer separation, is always related to the formation of vortices and to large energy losses in the wake of the body.

Let us consider the simplified boundary layer equation in order to investigate two-dimensional separation;

$$u \frac{\partial u}{\partial x} + v \frac{\partial u}{\partial y} = -\frac{1}{\rho} \frac{\partial P}{\partial x} + \nu \frac{\partial^2 u}{\partial y^2}$$

and define the separation as

$$\left(\frac{\partial u}{\partial y}\right)_{y=0} = 0$$

Since $u = v = 0$ at $y = 0$,

$$\nu \left(\frac{\partial^2 u}{\partial y^2}\right)_{y=0} = \frac{1}{\rho} \frac{\partial P}{\partial x}$$

The velocity profile in the boundary layer always has an inflection point in the region of decelerated flow and the velocity profile at separation point must have an inflection point. Thus, separation can occur only when the flow is decelerated. In two-dimensional separation, a bubble of fluid which has low velocity is always formed. This bubble is often unsteady and distinguished by interior streamlines which are closed loops or which extend to infinity.

There are two severe problems in boundary layer calculations when separation occurs.

1. The Goldstein singularity at the separation point in direct boundary layer calculations.
2. Numerical problems downstream of the separation point.

If a boundary condition prescribes the pressure gradient, then the boundary layer methods suffer from a singularity due to separation. Moreover, the singularity causes the numerical breakdown in direct boundary layer methods near the separation point. This Goldstein singularity can be overcome by using the displacement thickness or the wall shear stress, instead of the pressure gradient, for the boundary condition, which makes it possible to integrate the boundary layer equations through the separation point. Also, the full Navier-Stokes equations exhibit no singular behavior.

On the other hand, the boundary layer equations lead to a numerical instability in the region of reversed flow. The FLARE approximation is the most common method to overcome this instability. The momentum transport term $u\,\partial u/\partial x$ is deleted where u is smaller than zero. But the accuracy of this approximation decreases as the region of reversed flow increases. Therefore, it is necessary to introduce an upstream influence in that region. This is incorporated by the downstream upstream iteration procedure (DUIT) which consists of a sequence of alternating up- and downstream sweeps with the momentum transport term $u\,\partial u/\partial x$.

III. INTERACTION METHOD

A. INTRODUCTION

If the flow remains attached and the Reynolds number is high, the pressure distribution and the overall lift force can be obtained from a potential flow solution. Conventional boundary layer methods provide additional information about the skin friction distribution and the overall drag force. However, if the flow separates, no information is available for regions downstream of the separation point. Therefore, the overall forces cannot be obtained.

For this reason, interaction methods are introduced to overcome this problem. They provide a special coupling between the inner viscous and the outer inviscid flows, and can be classified as follows:

1. Weak interaction methods
    a. Direct method
    b. Inverse method
    c. Semi-inverse method
2. Strong interaction method

The weak interactions provide only a loose coupling between viscous and inviscid regions, i.e. two different regions are treated alternately. The viscous flow solver

deals with the flow in the viscous region and yields the boundary condition of the inviscid region, while the inviscid flow solver deals with the flow in the inviscid region and yields the boundary condition of the viscous region. The exchange of information through the boundary condition is slow, but regions such as those near separation and trailing edges require fast and direct coupling between viscous and inviscid region. While the strong interaction method treats displacement thickness and external velocity simultaneously, the weak interaction methods process one of these quantities as input and the other as output.

1. Inviscid flow methods
    a. Direct boundary conditions
        (1) Prescription of the airfoil shape
        (2) Zero normal velocity at the surface
    b. Inverse boundary conditions

        Prescription of a velocity distribution for the unknown airfoil shape
2. Viscous flow methods
    a. Direct boundary conditions
        (1) No slip condition requiring zero normal and zero tangential velocity at the surface.

(2) Prescription of the external velocity i.e. u-component of velocity at the edge of boundary layer

b. Inverse boundary conditions

(1) No slip condition

(2) Prescription of the displacement thickness

c. Boundary conditions for simultaneous interaction

(1) No slip condition

(2) Prescription of a linear combination of displacement thickness and external velocity

B. WEAK INTERACTION METHODS

1. Direct Method

A direct inviscid flow solver is combined with a direct viscous flow solver (see Figure 3.2). The boundary conditions are:

$$u(x,o) = 0 \quad v(x,o) = 0 \qquad (3.2)$$

$$u(x, y) = U_e(x)$$

This method is terminated at the point of vanishing skin friction. In the direct scheme, the pressure is calculated from the inviscid region, but the displacement thickness is determined from the viscous region. Because of

this phenomenon and Goldstein singularity, this method is not appropriate for flows with strong interference effects between viscous and inviscid regions.

2. Inverse Method

This method consists of an inverse inviscid and an inverse viscous flow solver (see Figure 3.3). The boundary conditions of the inverse boundary method are:

$$u(x,0) = 0 , \qquad v(x,0) = 0 \qquad (3.2)$$
$$\psi(x,y_e) = u(x,y_e)\left[y_e - \delta^*(x)\right]$$

where ψ is the stream function.

The roles of displacement thickness and external velocity distribution are exchanged in this method. The troubles related to the Goldstein singularity can be overcome, but the whole procedure takes a long time due to very slow convergence. Thus, this method can be applied to the regions of separated flow only and needs severe under-relaxation.

3. Semi-inverse Method

A direct inviscid flow solver is combined with an inverse viscous flow solver (see Figure 3.4). The input is the displacement thickness and the output is the external velocity distribution for both solvers. The two external velocity distributions are combined and then an updated displacement thickness is obtained through a relaxation procedure. A formula for satisfactory convergence is:

$$\delta^*_{new}(x) = \delta^*_{old}(x)\left[1 + w\left(\frac{U_{ev}(x)}{U_{eI}(x)} - 1\right)\right] \quad (3.3)$$

where w is the relaxation parameter.

The numerical weaknesses can be overcome, but the coupling is still loose.

C. STRONG INTERACTION METHOD

The simultaneous method solves the boundary layer equations subject to an interaction law (see Figure 3.5). Viscous displacement effects are allowed to cause substantial changes in the external velocity distribution. Since both displacement thickness and external velocity are treated as unknowns, one more additional relation, the so called interaction law, is needed. Thus the boundary conditions are:

$$u(x,0) = 0 \qquad v(x,0) = 0$$

$$\psi(x,y_e) = u(x,y_e)\left[y_e - \delta^* x\right] \quad (3.4)$$

$$u(x,y_e) = U_e^o(x) + 1/\pi \int_{x_1}^{x_2} \frac{d}{d\xi}\left[u(\xi,y_e)\,\delta^*(\xi)\right]\frac{d\xi}{x-\xi}$$

The last equation represents the interaction law.

Here, the external velocity for the boundary conditions can be written as:

$$U(x,y_e) = U_e(x) = U_e^o(x) + \Delta U_e(x) \quad (3.5)$$

where $U_e^o(x)$ is due to inviscid flow past the airfoil

$\Delta U_e(x)$ is the perturbation velocity due to the displacement effect of a boundary layer.

To obtain $\Delta U_e(x)$, the blowing velocity concept is used. Let us consider an airfoil along which sources are distributed (see Figure 3.1). This surface distribution of sources represents the effect of boundary layers. There are two ways to predict the displacement effect of a boundary layer on the outer inviscid flow:

1. Compute the inviscid flow past a displacement body
2. Replace the condition of zero normal velocity on the surface with a condition of prescribed blowing velocity at the surface

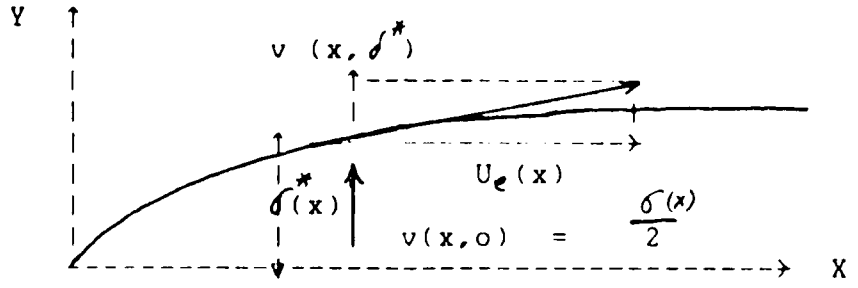

Figure 3.1 Blowing Velocity Concept

The streamlines are displaced away from the surface by the distributed sources which eject the fluid at the surface. Then the virtual displacement body becomes a streamline and the flow tangency condition is:

$$\frac{v\ (x, \delta^*)}{U_e(x)} = \frac{d\delta^*}{dx} \qquad (3.6)$$

From the thin airfoil approximation, the displacement thickness is assumed to be so small that u-component of velocity do not change across the layer and the airfoil in

this connection can be represented by a straight line. Therefore, the blowing velocity $v(x,0)$ is equal to half of the source strength $\sigma(x)$.

$$v(x,0) = 1/2\ \sigma(x) \tag{3.7}$$

$$v(x,0) = v(x,\delta^*) - \int_0^{\delta^*} \frac{\partial v}{\partial y}\, dy$$

$$= U_e \frac{d\delta^*}{dx} + \delta^* \frac{dU_e}{dx}$$

$$= \frac{d}{dx}(U_e \delta^*) \tag{3.8}$$

$$\text{Thus,} \quad \frac{d}{dx}(U_e \delta^*) = 1/2\ \sigma(x) \tag{3.9}$$

Now, the perturbation velocity due to the displacement effect can be written as:

$$\Delta U_e(x) = \frac{1}{2\pi} \int_{x_1}^{x_2} \frac{\sigma(\xi)}{x - \xi}\, d\xi \tag{3.10}$$

Finally, Eq. (3.6) becomes:

$$U_e(x) = U_e^o(x) + \frac{1}{2\pi} \int_{x_1}^{x_2} \frac{\sigma(\xi)}{x - \xi}\, d\xi \tag{3.11}$$

Eq. (3.11) represents the interaction law in usable form and the integral on the right hand side is known as the Hilbert integral.

In the simultaneous method, the inviscid flow solver provides an initial external velocity distribution, but the inviscid flow solver is not incorporated in the overall iteration process. Thus, the viscous flow solver needs the interaction law to obtain the necessary information about the inviscid region.

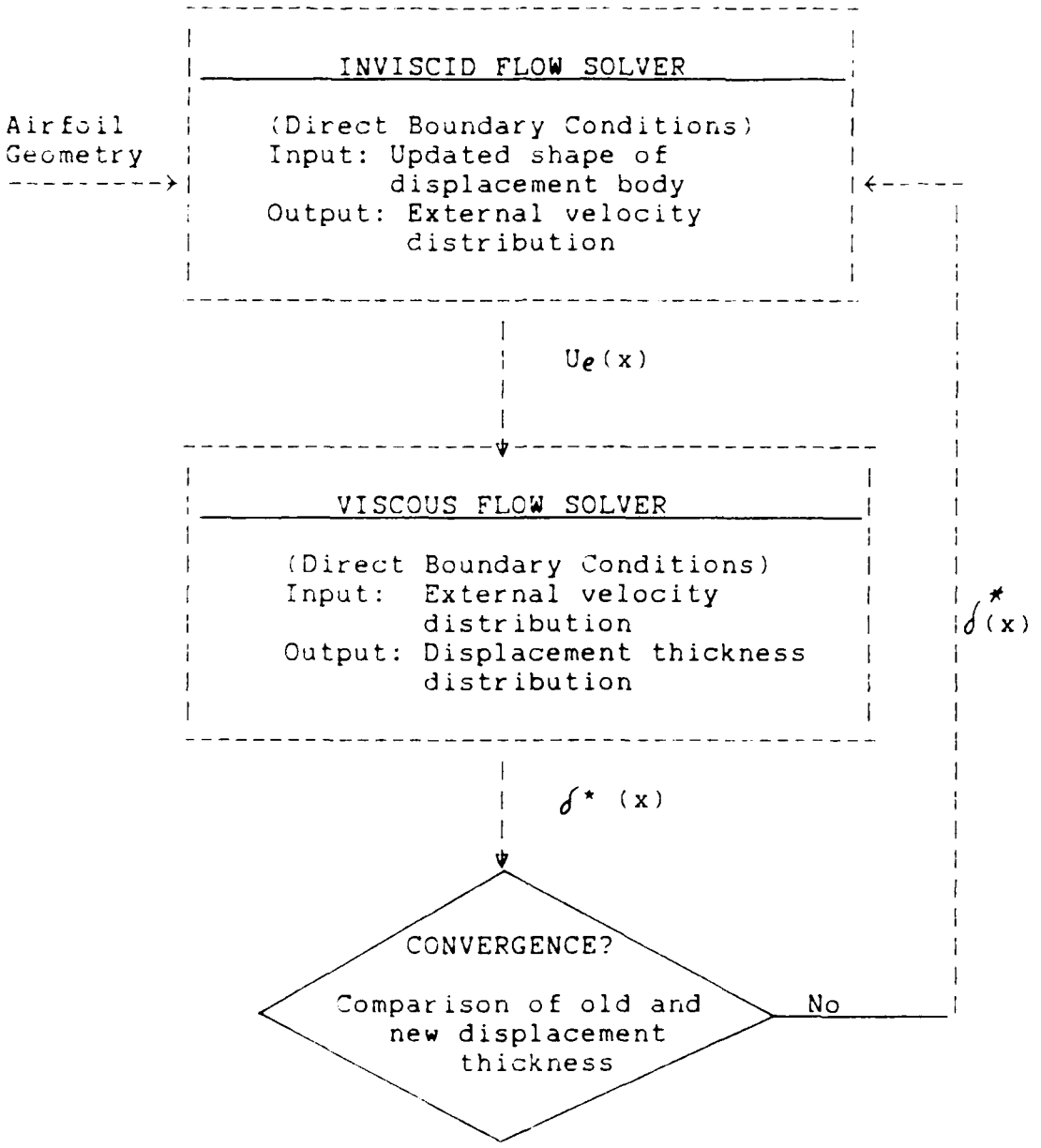

Figure 3.2 Direct Method

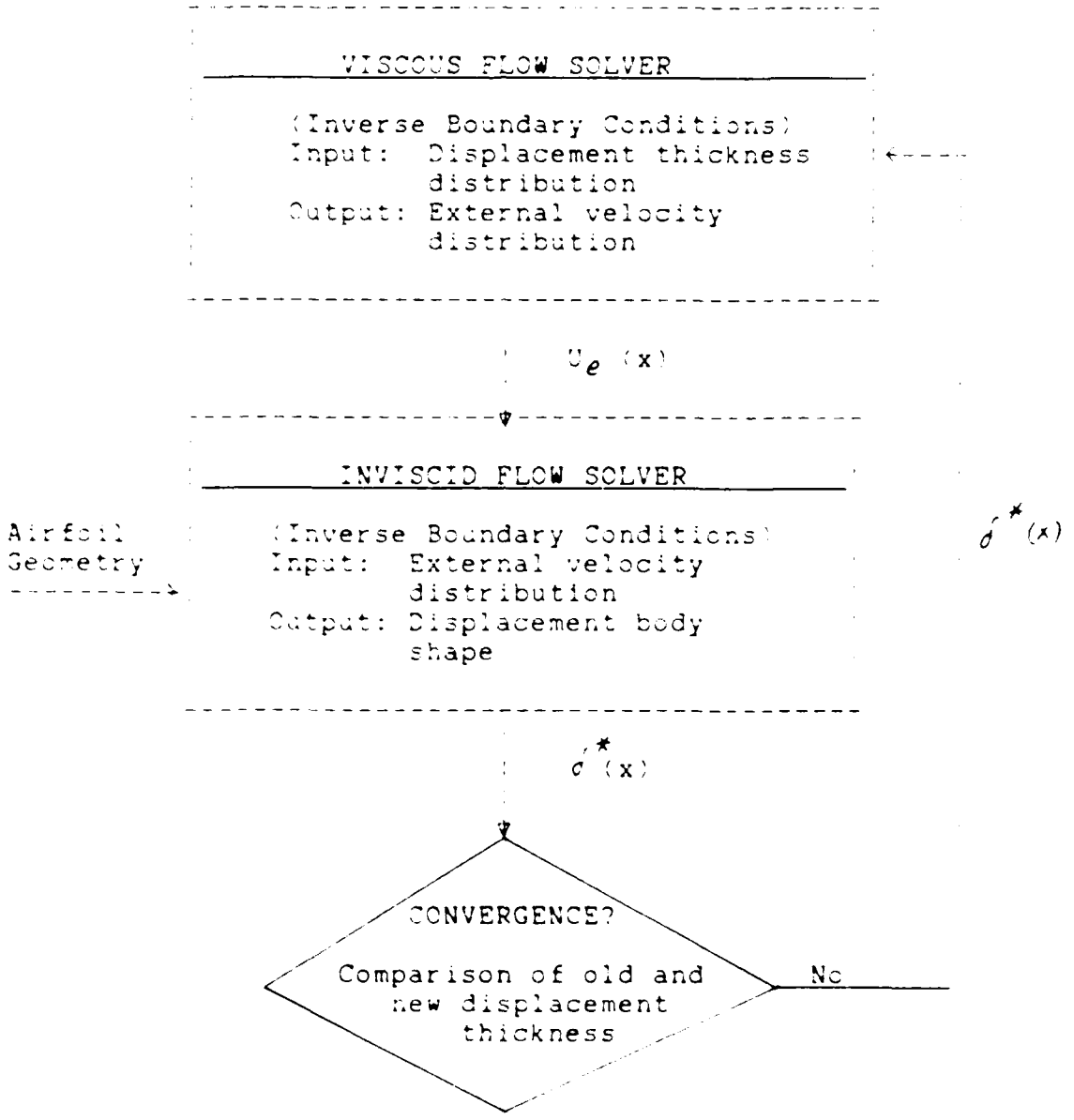

Figure 3.3 Inverse Method

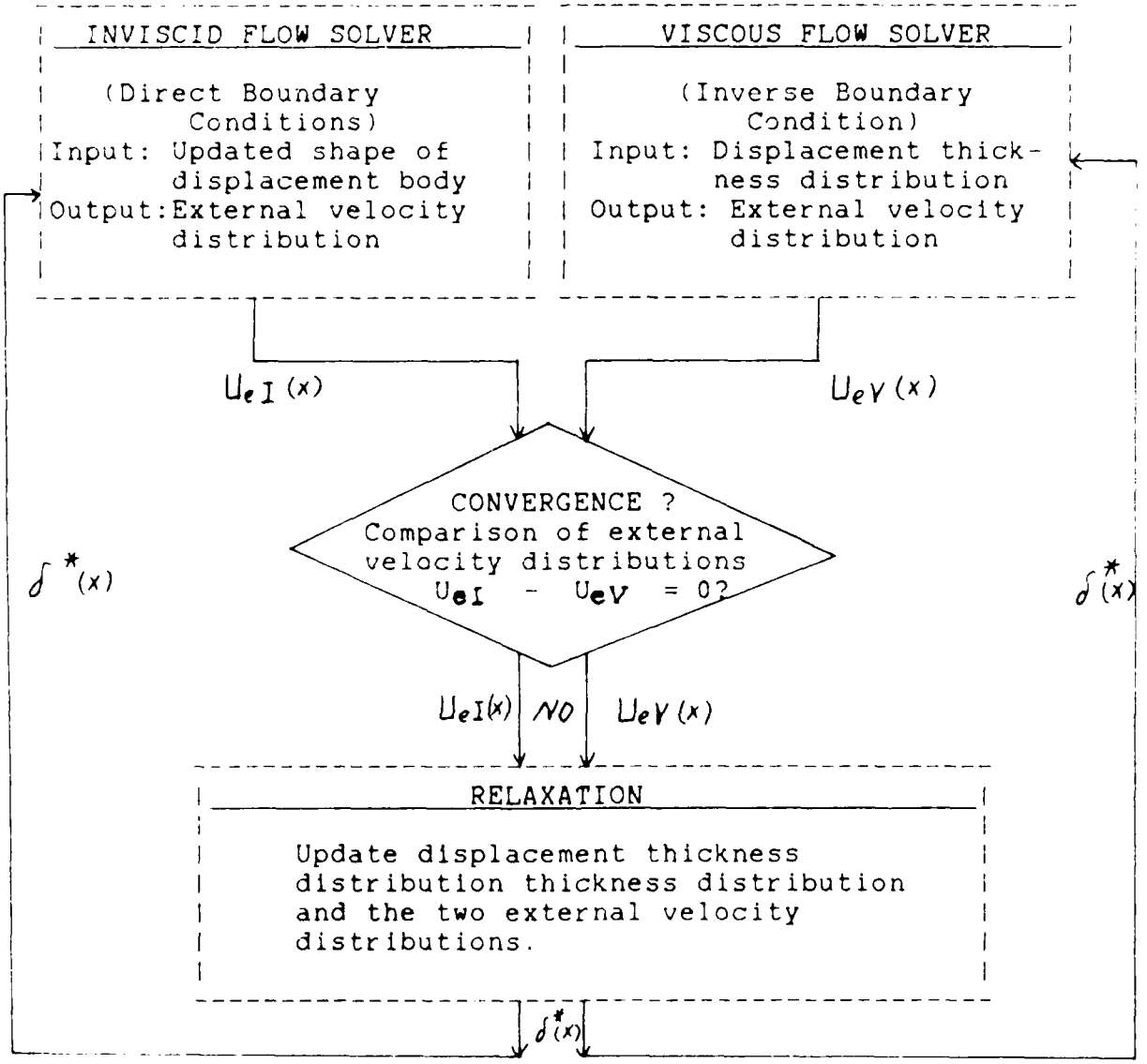

Figure 3.4 Semi-Inverse Method

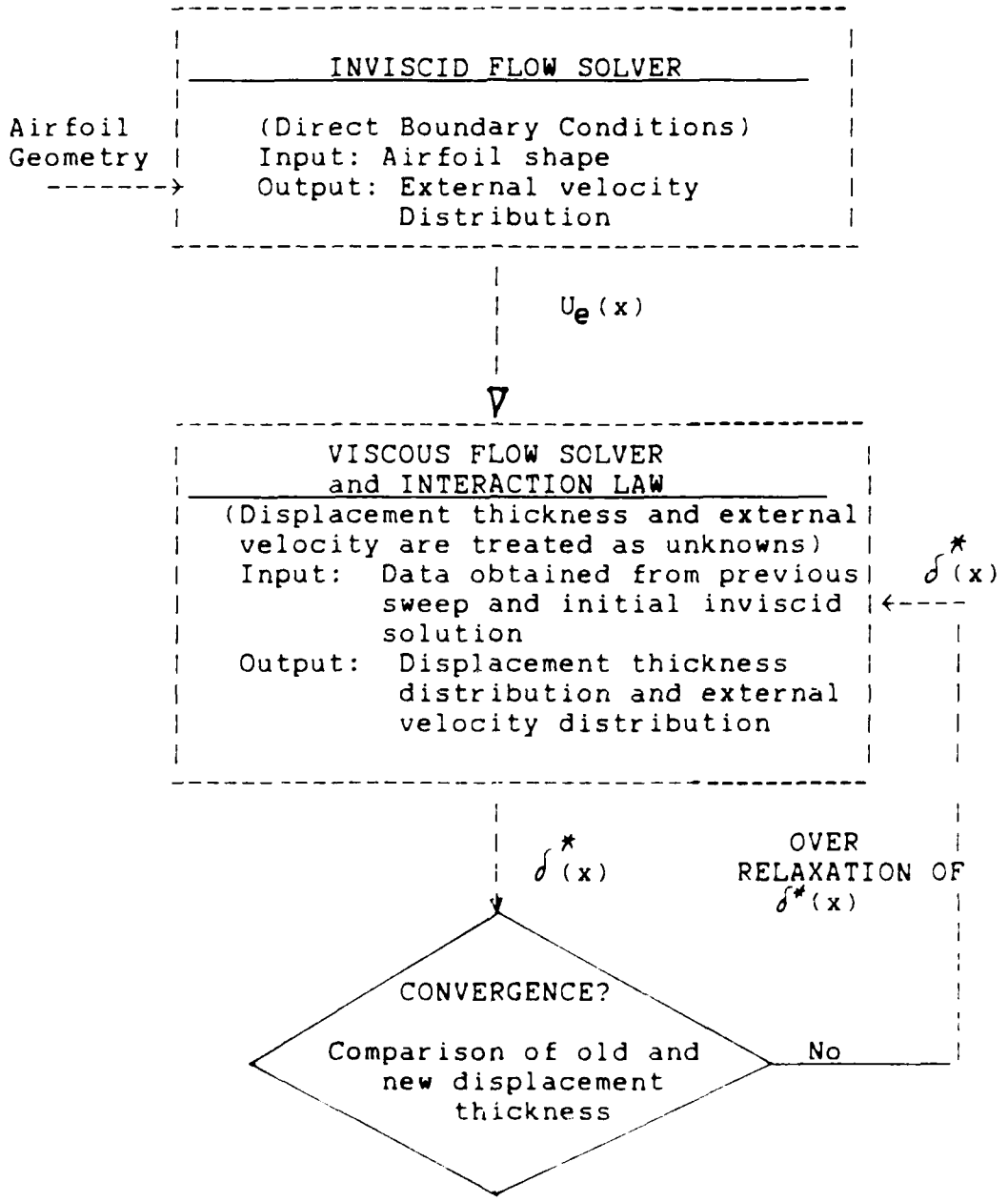

Figure 3.5 Simultaneous Method

IV. DESCRIPTION OF CEBECI'S INTERACTIVE PROGRAM

A. INPUT DESCRIPTION

1. Introduction

The Reynolds number is the most powerful parameter which can affect the flow. Wholly different flows can result from different Reynolds numbers (e.g. 6.0E + 06 against 0.28E + 06). Even though a flow with high Reynolds number behaves well and does not separate, it may have an extensive flow separation at a low Reynolds number. Numerical breakdown in boundary layer computations is partly due to this extensive flow separation at low Reynolds numbers. To avoid unrealistically large regions of flow separation, it is necessary to make some changes in the turbulence model for transitional flow. Reduction in transitional region to a proper level is a method to decrease numerical problems in computation. By doing this, more reasonable results can be obtained in low Reynolds number flows. Also, the computation at low Reynolds numbers needs more iterations to converge than at high Reynolds number, and the lift coefficient increases with Reynolds number at the same angle of attack because low Reynolds number flows exhibit a stronger displacement effect than high Reynolds number flows.

The results may be affected by transition location. The transition location can be either fixed by the user or computed from the following empirical formula given in Cebeci and Bradshaw (1977).

$$R_\theta = 1.174 \left(1 + \frac{22400}{R_x} \right) R_x^{0.46} \qquad (4.1)$$

Laminar flow separation, however, may occur upstream of the transition location predicted by the above equation. In this case, it is assumed that the onset of transition corresponds to the point of laminar separation, and the following message will be issued in the output:

TRANSITION LOCATION HAS BEEN RECOMPUTED AT THE POINT OF LAMINAR SEPARATION

The results of this program agree well with the experimental results up to stall at high Reynolds number flows. However, low Reynolds number flows may not agree well or experience numerical breakdown close to stall with the following messages:

at the very top of output,

+ IFY 002 I STOP 1

or at the very bottom of output,

IFY 207 I VFNTH: PROGRAM INTERRUPT (2)-
FLOATING-POINT EXCEPTION OVERFLOW

IFY 259 I STNCT: /ARG/ = /argument/,
(HEX = hexadecimal), APPROACHES SINGULARITY
or MAXIMUM NUMBER OF ITERATIONS EXCEEDED

Thus, the range of angle of attack should be considered carefully.

If the user requires many sweeps with IPRNT = 0 or 2, then the user needs to choose class "G" or "J" for enough running time and add additional command ", LINES = (m)" just after nnnnP on the following line to make enough space for print:

```
11* MAIN ORG = NPGVM1  nnnnP     , LINES = (m)
```

where nnnn is user's ID number.

m is the number of output lines in thousand

(Generally 10 is enough)

If the user does not do that, the following error message will be issued at the very top of the output and printing will be stopped abnormally:

```
IAT 1600 JOB number (user's job number) LINES EXCEEDED
IEF 450I  user's job number - ABEND S722 U0000
```

2. Detailed Input Data Description

The input to the computer program consists of 1 title line, 3 control lines and airfoil coordinate. User must follow the data format for specified column and type.

Title Line	FORMAT (18 A4)

This line provides any description as desired with any acceptable machine characters.

Control Line 1	FORMAT (5 I5)

Column	Name	Explanation
5	ITF(1)	Transition flag for the lower surface
10	ITF(2)	Transition flag for the upper surface = 1 Point of transition has to be specified by user. This option shall be used if experimental results are available or to avoid oscillations of the computed transition points. In the latter case, fix transition at the most upstream occurrence of computed transition. = 4 Point of transition will be calculated according to Eq. (4.1). No input is necessary for XTRL and XTRU. The computed point of transition will be redefined, if laminar separation takes place upstream of the location predicted by Eq. (4.1)
15	IRSTRT	Boundary layer restart flag.

	Read Starting Solution	Store Final solution or Unit 2
= 0	No	Yes
= 1	Yes	Yes

Leave 0 for general use

20	IGLMAX	Number of sweeps. Low Reynolds number flows need more sweeps to converge.
25	IPRNT	Print flag to control output print.

= -1 Summary print for the last two sweeps

= 0 Summary print for each sweep.

= 2 Whole print for all sweeps.

| Control Line 2 | FORMAT (4 E10.0)

Column	Name	Explanation
1 – 10	RL	Chord Reynolds number
11 – 20	XTRL	Fixed transition location for lower surface
21 – 30	XTRU	Fixed transition location for upper surface when the stagnation point is above the leading edge, XTRL may be positive. When the stagnation point is beneath the leading edge, XTRU may be negative.
31 – 40	ALPO	Angle of attack in degree

| Control Line 3 | FORMAT (I5)

Column	Name	Explanation
1 – 5	MPTS	Number of airfoil coordinates.

| Coordinate Data Line | FORMAT (2F 10.0)

Input dimensionless airfoil coordinates as two columns in one row (x/c, y/c). The order is trailing edge ⟶ lower surface ⟶ leading edge ⟶ upper surface ⟶ trailing edge. Thus, trailing edge is input twice.

B. OUTPUT DESCRIPTION

1. Introduction

To take the appropriate results from the output, user must check the convergence. This can be done by comparing the convergence indicators, lift coefficient and displacement thickness at trailing edge, when the computation is completed successfully for the given sweeps. If the convergence indicators show steady values over some sweeps i.e. each difference of the convergence indicators is less than 1%, the results are considered as converged.

Sometimes, the user may experience failure in computations at low Reynolds numbers and high angles of attack due to numerical breakdowns. These breakdowns take place when Newton iteration does not converge near to the trailing edge on the upper surface or the computation is terminated by Fortran error with this message:

IFY 251I SSQRT; ARG = argument, LESS THAN ZERO

Also, extensive flow separation cause numerical breakdowns of the boundary layer computation. These unrealistically large regions of separation at low Reynolds numbers can be reduced by changing the transitional flow model.

2. Detailed Output Data Description

The output of the computer program for IPRNT = 1

and 0 can be divided into three parts as follows:

1. Input data and inviscid lift coefficient
2. Alternating boundary layer parameters for each surface and wake.
3. Inviscid and viscous pressure distributions

The following is the list of computed boundary layer parameters in the order in which they appear in the output print.

Name in print	Name in program	Definition	Explanation
X(NX)	X(I)	$\frac{\xi}{c}$	Dimensionless surface distance from the stagnation point
X/C(NX)	XC(I)	$\frac{X}{c}$	Dimensionless chordwise distance from leading edge
V(1,NX)	VWL(I)	$\left(\frac{d^2 f}{d \eta^2}\right)_w$	Dimensionless wall shear stress parameter.
CF	CF(I)	$\frac{2 \tau_w}{\rho U_e^2}$	Local skin friction coefficient
DELST	DLS(I)	$\frac{\delta^*}{c}$	Dimensionless displacement thickness. $\delta^* = \int_0^\infty \left(1 - \frac{u}{U_e}\right) dy$
THETA	THETA(I)	$\frac{\theta}{c}$	Dimensionless momentum thickness $\theta = \int_0^\infty \frac{u}{U_e}\left(1 - \frac{u}{U_e}\right) dy$
UE(NX)	UE(I)	$\frac{U_e I}{U_\infty}$	Dimensionless external velocity computed from the inviscid method with viscous effect.

W(NP,NX)	WNP(I)	$\frac{U_e V}{U_\infty}$	Dimensionless external velocity computed from the interactive boundary layer method.
D(NX)	D(KX)	$\frac{U_{ev}}{U_\infty}\ \frac{\delta^* \sqrt{RL}}{c}$	Product of velocity and displacement thickness in dimensionless form for the current sweep (D), from the previous sweep (DB). D and DB are printed in the output as updated values through the relaxation procedure
DB(NX)	DB(KX)		

$$\delta_{new}(NX) = \delta_{old}(NX)\left[1 + \omega\left(\frac{W(NP,NX)}{UE(NX)} - 1\right)\right]$$

IT	ITN(I)	Iteration count for the convergence of solutions at a given NX-station.
NP	NNP(I)	Number of points across the boundary layer.

C. HOW TO CHANGE THE ORIGINAL PROGRAM

Cebeci's computer program is written entirely in FORTRAN and consists of the following eight FORTRAN files:

FILE 1 FORTRAN A1

FILE 2 FORTRAN A1

FILE 3 FORTRAN A1

FILE 4 FORTRAN A1

~~FILE 5 FORTRAN A1~~

FILE 6 FORTRAN A1

FILE 7 FORTRAN A1

FILE 8 FORTRAN A1

FILE 9 FORTRAN A1

Also, the user needs the following six JCL files to run changed program:

QUEST 1	JCL	A1
ALLPDS	JCL	A1
QUEST 3	JCL	A1
STOPDS	JCL	A1
LOADMOD	JCL	A1
INTAPCLG	JCL	A1

"QUEST 1" lists all data set on MSS (Mass Storage System) that belong to student user ID number and in group PUB4B (public disk volume), which deletes the data set 180 days after creation.

"ALLPDS" allocates space for a PDS (partitioned Data Set) on PUB4B prior to reading a data set into it, using the utility program IEFBR 14 which pre-allocates or deletes data sets.

"QUEST 3" lists the members of a PDS and calculates the remaining available space within the data set.

"STOPDS" places a FORTRAN source file in a PDS.

The SYSUT2 DD statement describes the output data set and the SYSUT1 DD statement describes the input data set.

"LOADMOD" creates a load module.

"INTAPCLG" compiles source code, loads and executes text file.

A list of all JCL files is given at the end of this chapter and more information is in the User's Guide to MVS at NPS (1986).

The following is the procedure to change the program and run it:

Step 1

1. Make changes in FORTRAN files as required. Remember those eight FORTRAN files compose one program. Thus, the user must check all files which are related to changes.

2. Review and update FORTRAN errors, if necessary.

Step 2

1. Change job name "xxxxxx", user ID number "nnnn" and library name "yyy" with user's own in all JCL files to make them be the user's.

2. Submit four JCL files:
"QUEST1" "ALLPDS" "QUEST 3" "LOADMOD".

Step 3

Do the following for all FORTRAN files to submit them to user's library.

1. Open "STOPDS" JCL file.

2. Change the FORTRAN file number indicated by n on the sixth line.

```
//SYSUT2 DD DISP --- YYYLIB (INTAIR n)
```

3. Insert the FORTRAN file between
"//SYSUT1 DD, *" and "/*".

4. Submit "STOPDS" JCL file.

5. Check the result by any error message at the very top and bottom part and condition code.

6. Update errors, if necessary.

Step 4

Do the following to run the changed program.

1. Open "INTAPCLG" JCL file.

2. Insert the input data between

"//GO. SYSIN DD * " and "/*".

3. Submit "INTAPCLG" JCL file

From the second change, do steps 1, 3 and 4.

D. APPLICATION OF CEBECI'S PROGRAM

Cebeci's interactive program was applied to a single airfoil, FX 63 -137, at three Reynolds numbers. The print flag is 0 and the number of airfoil coordinates is 49 for all cases. The results are compared with experimental data and the turbulence model has been changed to get better results. The experimental results are taken from Reference 3.

Figure 4.2 and 4.3 show the comparison of lift and drag coefficients for three Reynolds numbers. Drag coefficients are computed at the trailing edge. It is seen that the results are closer to the experimental data as the Reynolds number increases.

Figures 4.4, 4.5 and 4.6 show the skin friction coefficients on the upper and lower surfaces as a function of angle of attack for the same three Reynolds numbers. Legends indicate the angle of attack. As the Reynolds number increases, the length of the separation bubble decreases on both surfaces for the same angle of attack. Especially, Figure 4.4, which has a different label of y-axis from the other figures, indicates an unrealistic flow on the upper surface at low Reynolds number. In Figure 4.5 and 4.6, however, the flow on the upper surface is separated from about 80% chord at all angles of attack.

Figures 4.7, 4.8 and 4.9 present how the displacement thickness varies according to the angle of attack and the Reynolds number. As the Reynolds number increases, the displacement thickness decreases on both surfaces. As the angle of attack increases, it also increases on the upper surface, but decreases on the lower surface.

Table 4.1 represents the computed and fixed transition locations which are used in Figures 4.10 - 4.13. The computed transition locations XTRL = 0.288922 at ALPD = 8 degrees and XTRL = 0.206866 at ALPD = 10 degrees were printed incorrectly. In this case, the correct transition locations can be obtained by the following procedure:

1. Calculate the difference of XTRL's at ALPD = 4 degrees and 6 degrees.
2. Add the difference to XTRL of ALPD = 6 degrees and

take the result as a temporary XTRL for ALPD = 8 degrees.

3. Fix transition location with the temporary XTRL

4. Run the program to print XC(I), GAMTR(I) from SUBROUTINE OUTPUT in FILE 3 FORTRAN A1.

5. Take XC(I), where the value of GAMTR(I) is finally equal to zero, as the correct transition location.

6. From the same procedures with XTRL's at ALPD = 6 degrees and 8 degrees, obtain the correct transition location for ALPD = 10 degrees.

Figures 4.10 ~ 4.13 show the effect of variations in the empirical constant, $G_{\gamma_{tr}}$, in turbulence model at R_e = 0.28 x 10^6 . In the legend of Figures 4.10 and 4.11, the three numbers are the values of the empirical constant, C means that the transition location is computed by Eq. (4.1) and F means that it is fixed. The lift curve is closer to the experimental data as the empirical constant decreases, but the drag curve is closest when the empirical constant is 120.

The reason why we can obtain better results by reducing the empirical constant is shown in Figure 4.12 and 4.13. GAMMATR (γ_{tr}) is the intermittency factor which is a function of the x-coordinate with values 0.0 at the beginning point of transition and 1.0 at the ending point of transition. The intermittency factor makes it possible to avoid a sudden transition from laminar to turbulent by smoothing out the step-shaped change of viscosity from kinematic to eddy. The relation between the empirical

constant and the intermittency factor is given as:

$$\gamma_{tr} = 1 - \exp\left[- \frac{(x - x_{tr})\, Ue^{3}\, Re_{x_{tr}}^{-1.34}}{G_{\gamma_{tr}}} \int_{x_{tr}}^{x} \frac{1}{Ue}\, dx \right]$$

where, x_{tr} denotes the beginning point of transition.

The transition length is mainly determined by the empirical constant $G_{\gamma_{tr}}$ which is set as 1200 in Cebeci's original program. Decreasing the value of the empirical constant reduces the transition length. In this way, the unrealistic flow shown in Figure 4.4 can be avoided and more reasonable results, which are closer to the experimental data, can be obtained. In Figure 4.12 and 4.13, the legend indicates the angle of attack, and each of four line patterns is used twice for two angles of attack (e.g. —; - 4 degrees and 4 degrees). The direction of curves, as the angle of attack increases, is from right to left at the upper surface (Figure 4.12) and from left to right at the lower surface (Figure 4.13).

List of JCL Files

******* ALLPDS JCL A1 *******

```
//XXXXXX    JOB (NNNN,9999),'ALLOCATE PDS',CLASS=A
//*MAIN ORG=NPGVM1.NNNNP
//        EXEC  PGM=IEFBR14
//SYSPRINT DD SYSOUT=A
//DD1 DD UNIT=3330V,MSVGP=PUB4B,DISP=(NEW,CATLG,DELETE),
//        SPACE=(CYL,(4,4,6)),DSN=MSS.SNNNN.YYYLIB
//
```

******* QUEST1 JCL A1 *******

```
//XXXXXX    JOB (NNNN,9999),'QUESTION',CLASS=A
//*MAIN ORG=NPGVM1.NNNNP
//  EXEC PGM=IDCAMS
//SYSPRINT DD SYSOUT=A
//SYSIN    DD *
 LISTDSET GROUP(PUB4B) LEVEL(MSS.SNNNN)
/*
//
```

******* QUEST3 JCL A1 *******

```
//XXXXXX    JOB (NNNN,9999),'LIST',CLASS=A
//*MAIN ORG=NPGVM1.NNNNP
//  EXEC PGM=IEHLIST
//SYSPRINT DD SYSOUT=A
//DD1 DD UNIT=3330V,VOL=SER=MS0005,DISP=SHR
//SYSIN    DD *
 LISTVTOC FORMAT,VOL=3330V=MS0005,DSNAME=MSS.SNNNN.YYYLIB
 LISTPDS  VOL=3330V=MS0005,DSNAME=MSS.SNNNN.YYYLIB
/*
//
```

******* STOPDS JCL A1 *******

```
//XXXXXX    JOB (NNNN,9999),'PLACE PDS'
//*MAIN ORG=NPGVM1.NNNNP
//        EXEC  PGM=IEBGENER
//SYSPRINT DD SYSOUT=A
//SYSIN    DD DUMMY
//SYSUT2   DD DISP=(OLD,KEEP),DSNAME=MSS.SNNNN.YYYLIB(INTAIR_),
//            DCB=(RECFM=FB,LRECL=80,BLKSIZE=8000)
//SYSUT1   DD *
/*
//
```

```
  *******  LOADMOD  JCL  A1  *******

//XXXXX    JOB (NNNN,9999),'CREATE LOADMODULE',CLASS=C
//*MAIN ORG=NPGVM1.NNNNP
//        EXEC  FORTVCL,PARM.FORT='LVL(77),NOS,NOX,NOMAP'
//FORT.SYSPRINT DD DUMMY
//FORT.SYSIN    DD DISP=SHR,DSN=MSS.SNNNN.YYYLIB(INTAIR1)
//               DD DISP=SHR,DSN=MSS.SNNNN.YYYLIB(INTAIR2)
//               DD DISP=SHR,DSN=MSS.SNNNN.YYYLIB(INTAIR3)
//               DD DISP=SHR,DSN=MSS.SNNNN.YYYLIB(INTAIR4)
//               DD DISP=SHR,DSN=MSS.SNNNN.YYYLIB(INTAIR6)
//               DD DISP=SHR,DSN=MSS.SNNNN.YYYLIB(INTAIR7)
//               DD DISP=SHR,DSN=MSS.SNNNN.YYYLIB(INTAIR8)
//               DD DISP=SHR,DSN=MSS.SNNNN.YYYLIB(INTAIR9)
//LKED.SYSLMOD DD DISP=SHR,DSN=MSS.SNNNN.YYYLIB(INTCAS)
//LKED.SYSIN DD DSN=NULLFILE
//


  *******  INTAPCLG  JCL  A1  *******

//XXXXXX    JOB (NNNN,9999),'COMP LOAD AND GO',CLASS=G
//*MAIN ORG=NPGVM1.NNNNP
//        EXEC  FORTVCLG,PARM.FORT='LVL(77),NOS,NOX,NOMAP',
//        REGION.GO=1280K
//FORT.SYSPRINT DD DUMMY
//FORT.SYSIN    DD DISP=SHR,DSN=MSS.SNNNN.YYYLIB(INTAIR1)
//               DD DISP=SHR,DSN=MSS.SNNNN.YYYLIB(INTAIR2)
//               DD DISP=SHR,DSN=MSS.SNNNN.YYYLIB(INTAIR3)
//               DD DISP=SHR,DSN=MSS.SNNNN.YYYLIB(INTAIR4)
//               DD DISP=SHR,DSN=MSS.SNNNN.YYYLIB(INTAIR6)
//               DD DISP=SHR,DSN=MSS.SNNNN.YYYLIB(INTAIR7)
//               DD DISP=SHR,DSN=MSS.SNNNN.YYYLIB(INTAIR8)
//               DD DISP=SHR,DSN=MSS.SNNNN.YYYLIB(INTAIR9)
//LKED.SYSPRINT DD DUMMY
//LKED.SYSIN    DD DSN=NULLFILE
//GO.FT01F001 DD UNIT=SYSDA,SPACE=(CYL,(1,1))
//GO.FT02F001 DD UNIT=SYSDA,SPACE=(CYL,(1,1))
//GO.FT03F001 DD UNIT=SYSDA,SPACE=(CYL,(1,1))
//GO.FT04F001 DD UNIT=SYSDA,SPACE=(CYL,(1,1))
//GO.FT99F001 DD UNIT=SYSDA,SPACE=(CYL,(1,1))
//GO.FT08F001 DD UNIT=SYSDA,SPACE=(CYL,(1,1))
//GO.FT09F001 DD UNIT=SYSDA,SPACE=(CYL,(1,1))
//GO.FT10F001 DD UNIT=SYSDA,SPACE=(CYL,(1,1))
//GO.FT11F001 DD UNIT=SYSDA,SPACE=(CYL,(1,1))
//GO.FT06F001 DD SYSOUT=A
//GO.SYSIN    DD *
/*
//
```

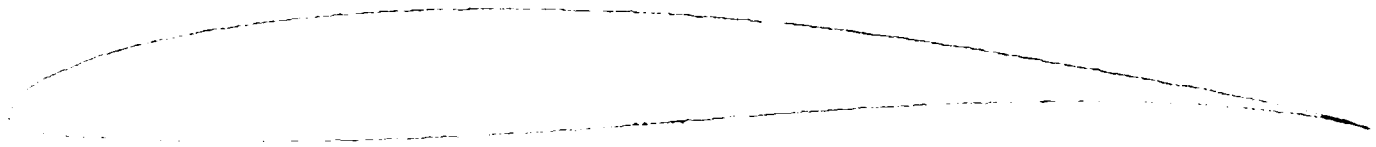

Figure 4.1 EX 63 - 137

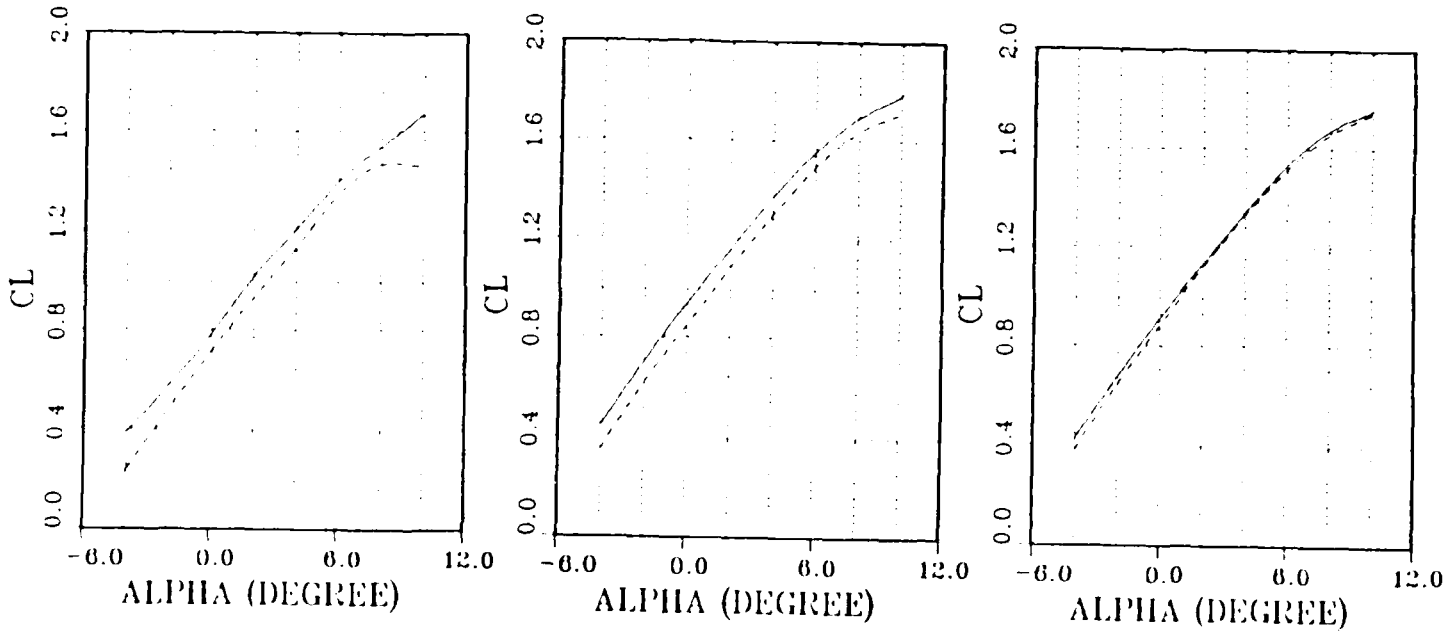

(a) Re = 0.28 x 10^6 (b) Re = 0.5 x 10^6 (c) Re = 0.7 x 10^6

Figure 4.2 Lift Versus Angle Of Attack

——— : Experimental
----- : Interaction method

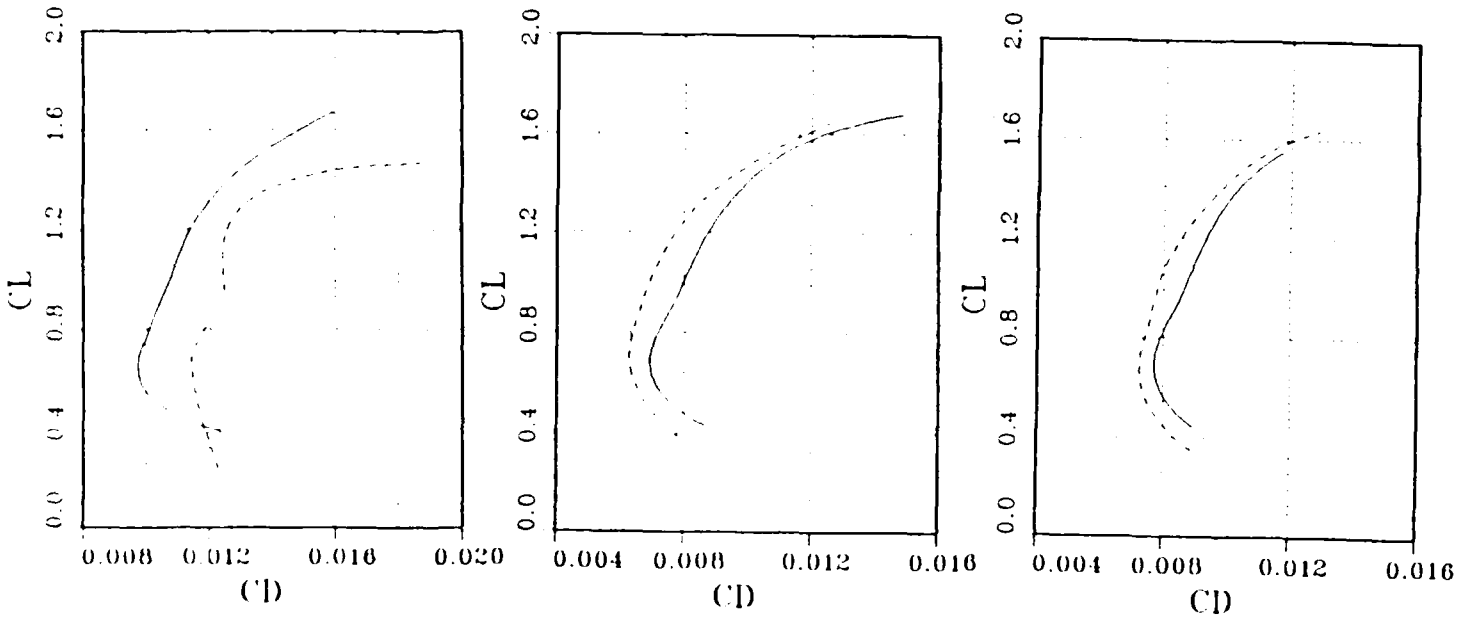

(a) Re = 0.28 x 10^6 (b) Re = 0.5 x 10^6 (c) Re = 0.7 x 10^6

Figure 4.3 Lift Versus Drag

——— : Experimental
----- : Interaction method

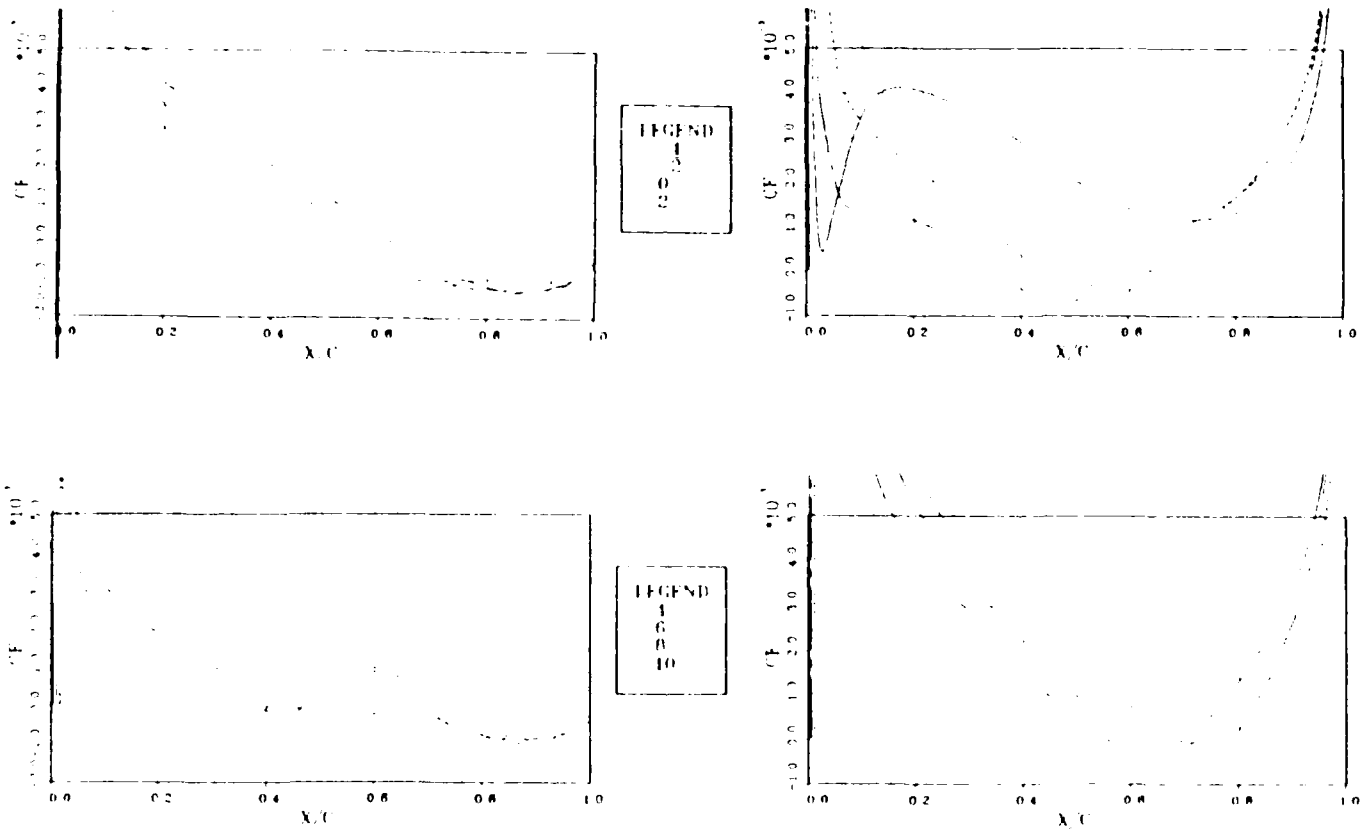

(a) Upper surface

(b) Lower surface

Figure 4.4 Variation Of Local Skin Friction Coefficients ($Re = 0.28 \times 10^6$)

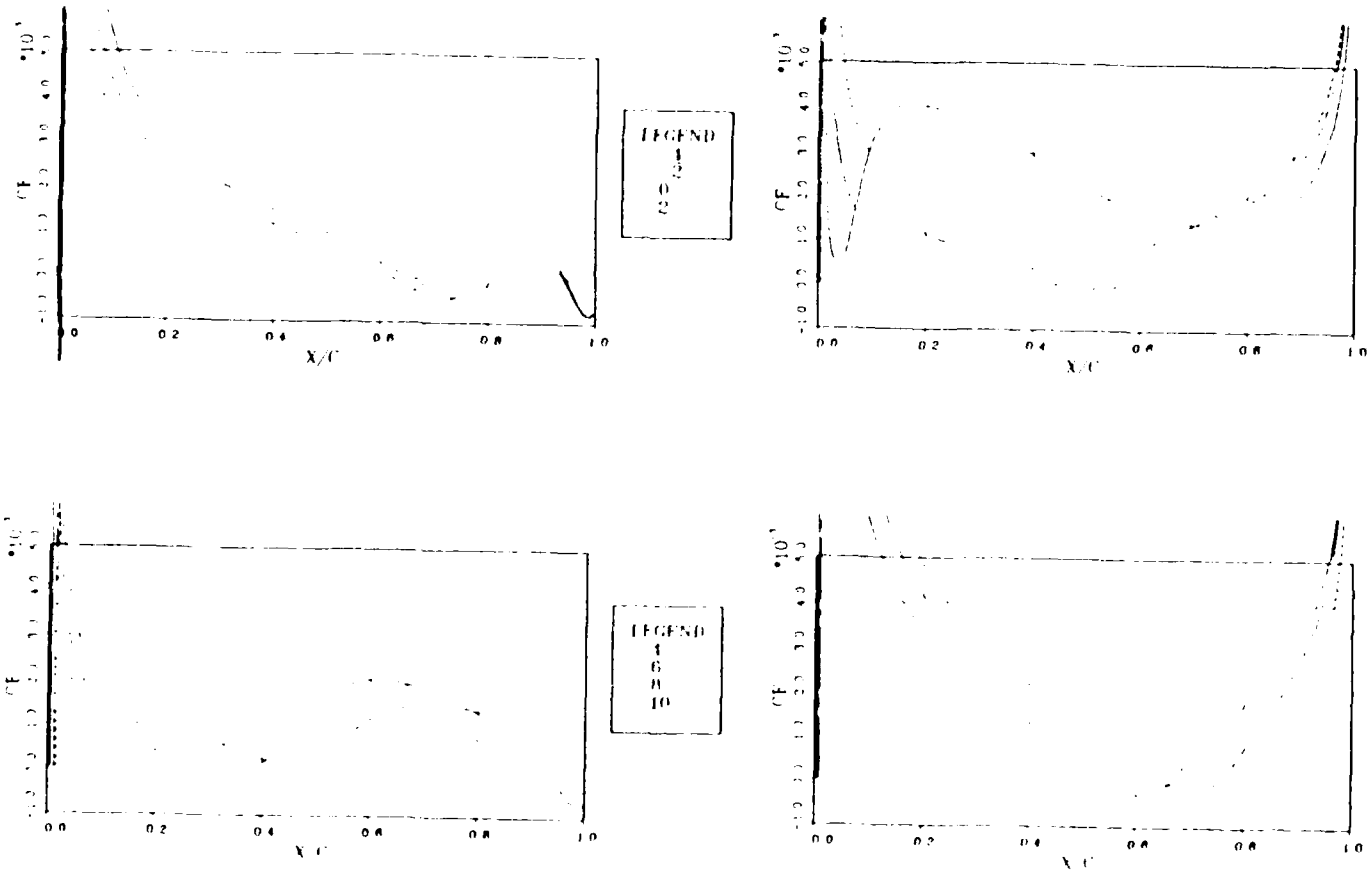

(a) Upper surface

(b) Lower surface

Figure 4.5 Variation Of Local Skin Friction Coefficients (Re = 3.5 x 10^6)

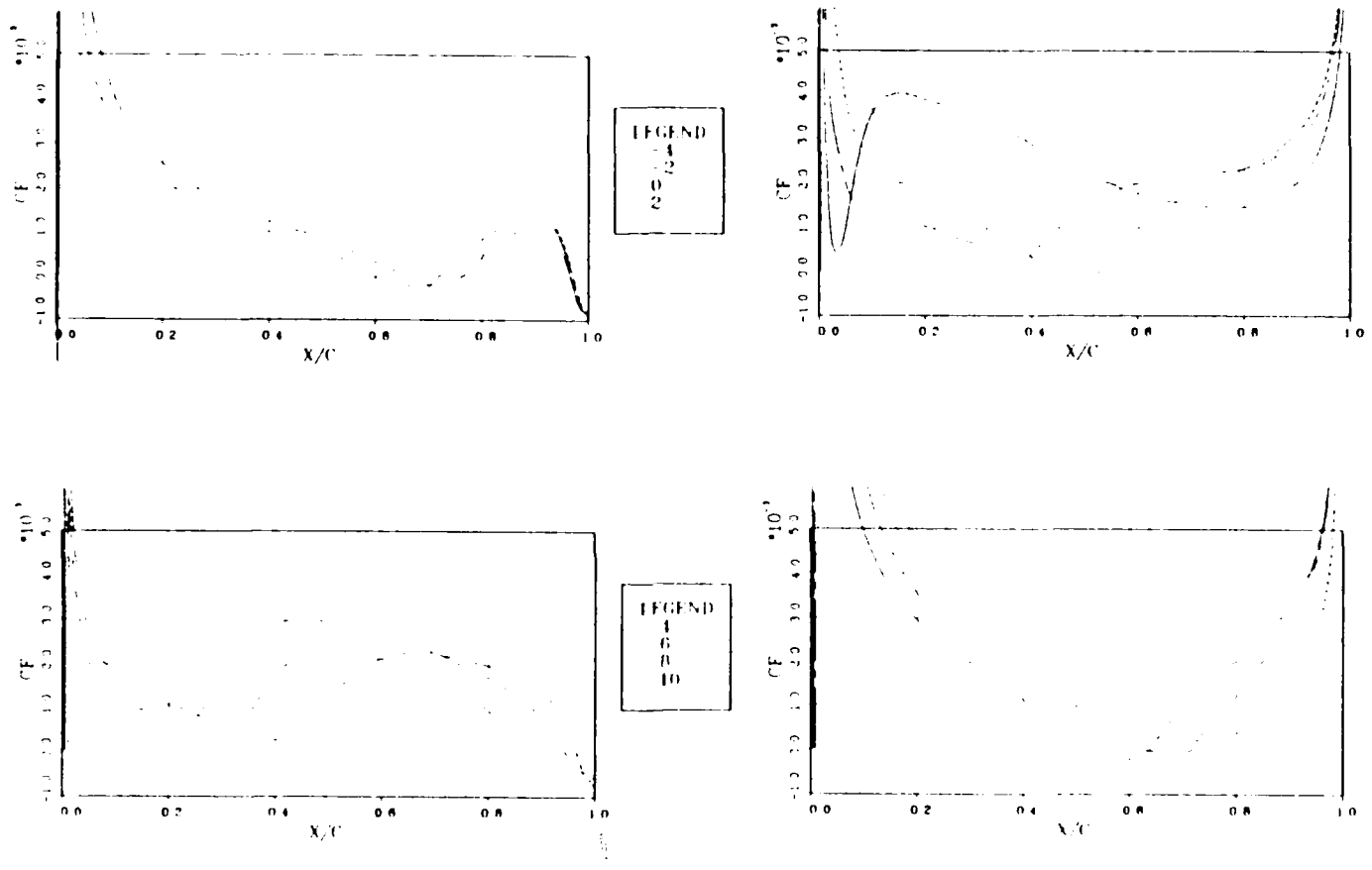

(a) Upper surface

(b) Lower surface

Figure 4.6 Variation Of Local Skin Friction Coefficients (Re = 0.7 x 10^6)

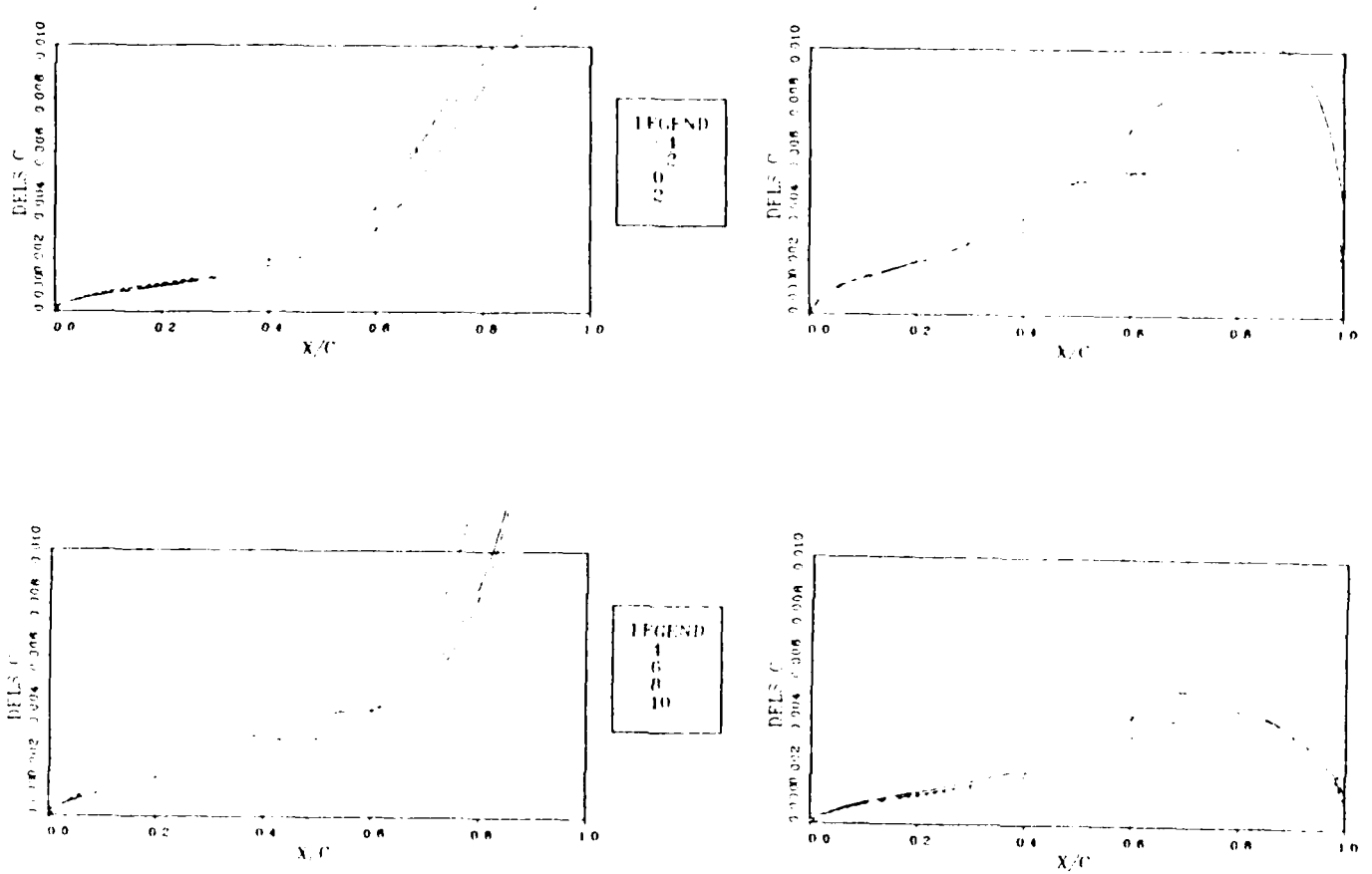

(a) Upper surface

(b) Lower surface

Figure 4.7 Distribution Of Displacement Thickness

(Re = 0.28×10^6)

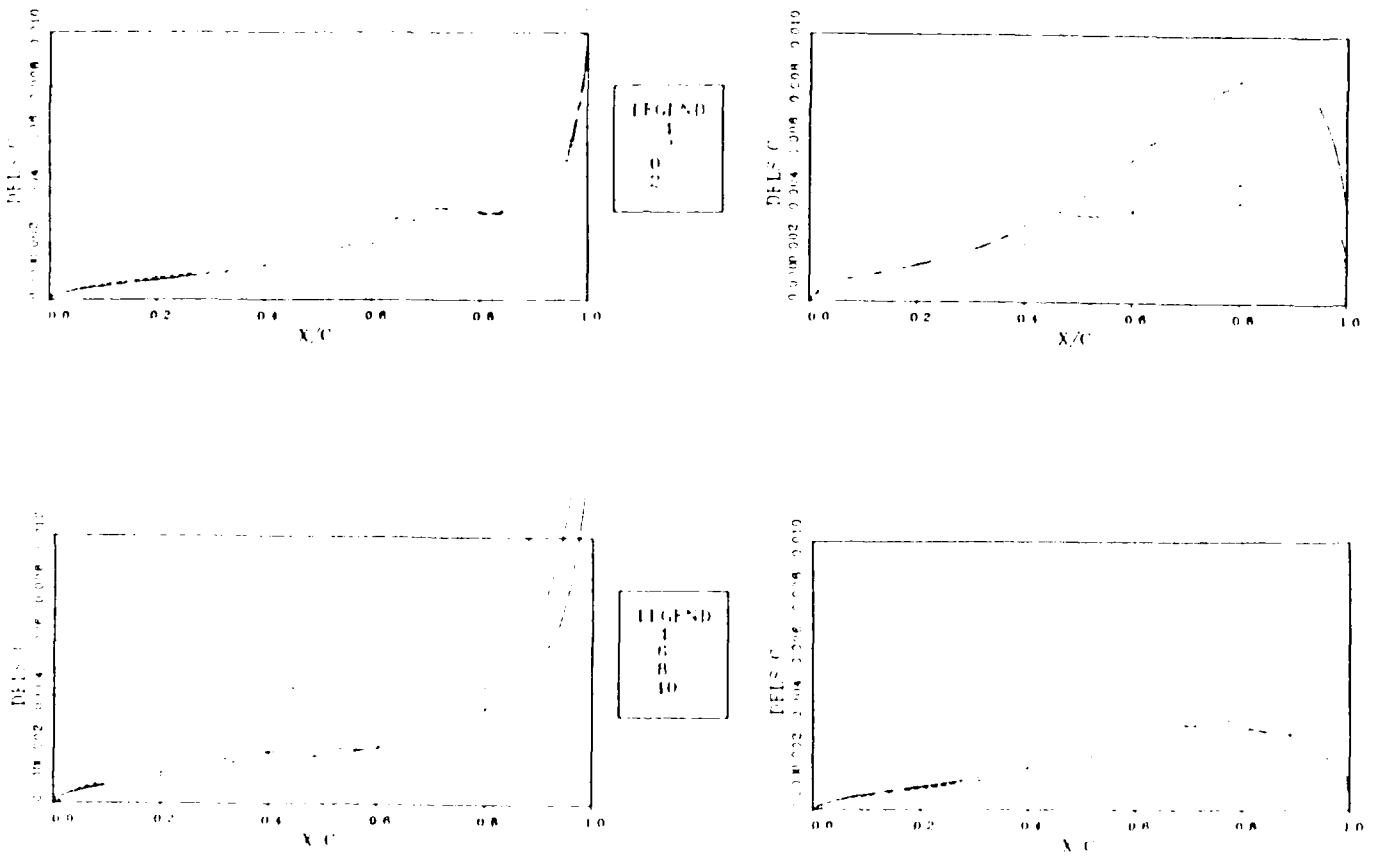

(a) Upper surface (b) Lower surface

Figure 4.8 Distribution Of Displacement Thickness
(Re = 0.5 x 10^6)

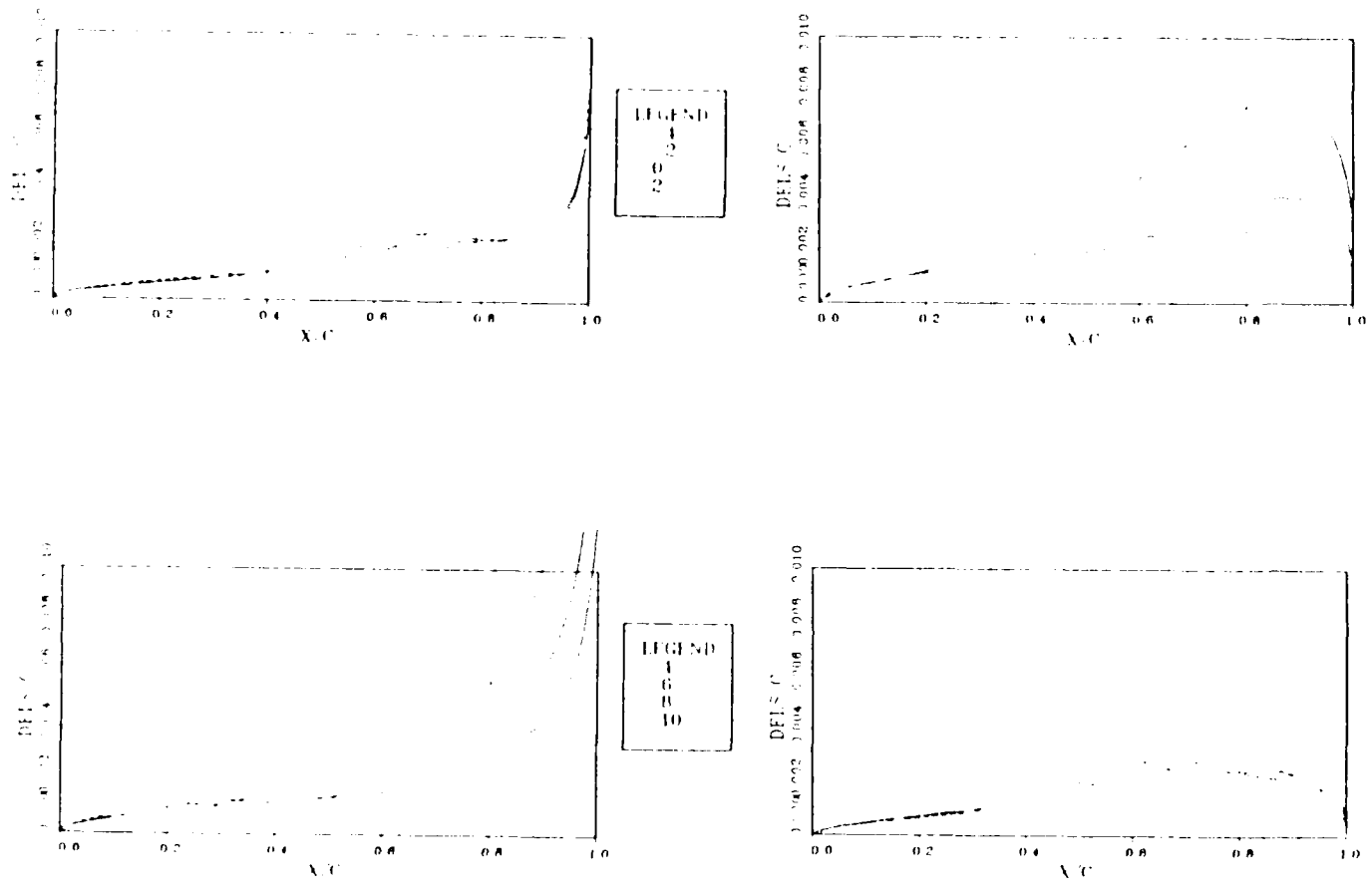

(a) Upper surface

(b) Lower surface

Figure 4.9 Distribution Of Displacement Thickness

(Re = 0.7 x 10^6)

TABLE 4.1 TRANSITION LOCATION

ALPD	COMPUTED		FIXED	
	XTRL	XTRU	XTRL	XTRU
-4	0.010680	0.584178	0.010680	0.584178
-2	0.326179	0.542882	0.326179	0.542882
0	0.391919	0.501232	0.391919	0.501232
2	0.458252	0.478890	0.458252	0.459243
4	0.524927	0.416490	0.524927	0.416490
6	0.632658	0.353115	0.632385	0.353115
8	0.288922	0.288922	0.676143	0.288922
10	0.206866	0.224747	0.718631	0.206866

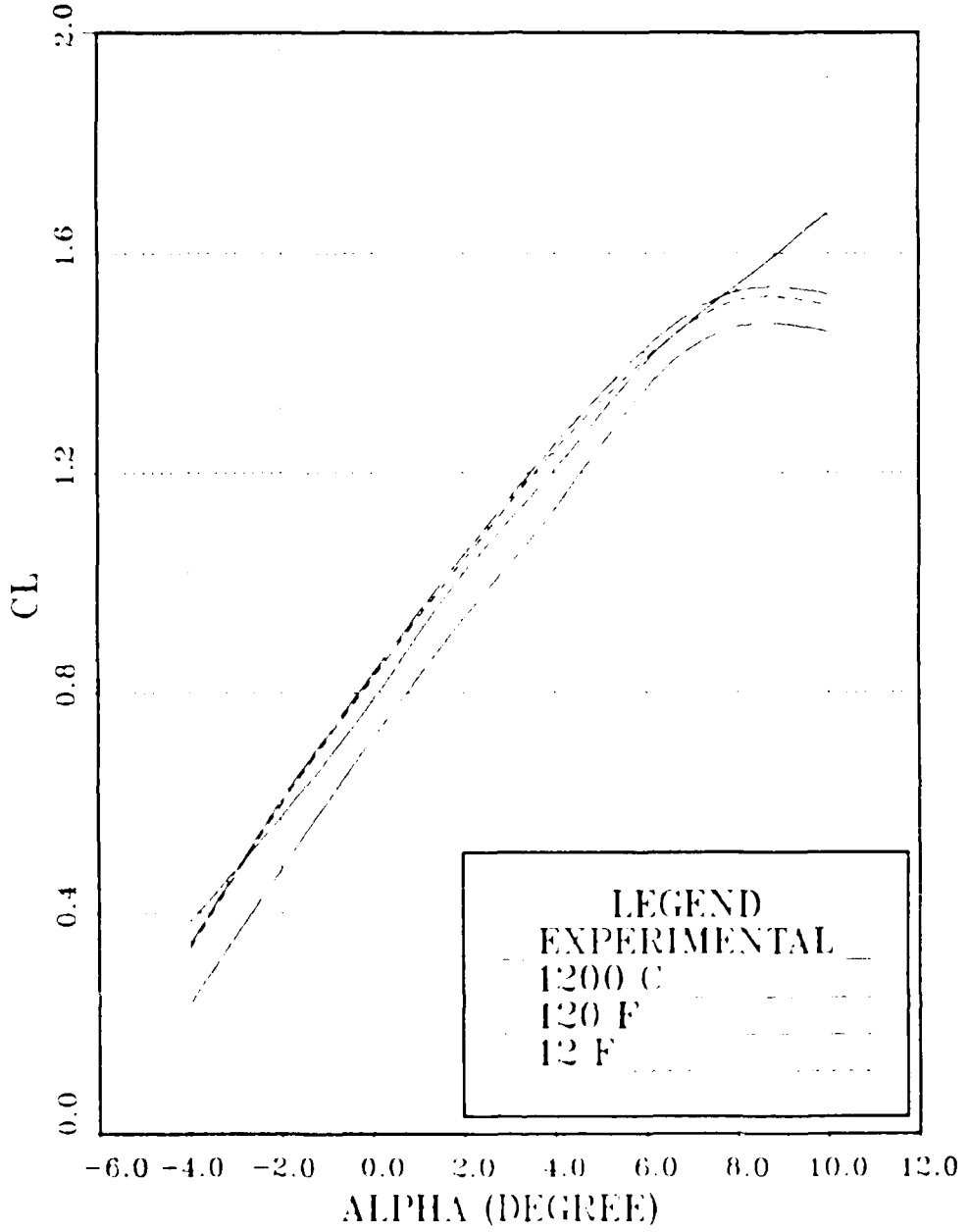

Figure 4.10 Comparison of Lift Curves
for Different Empirical
Values of γ_{tr}

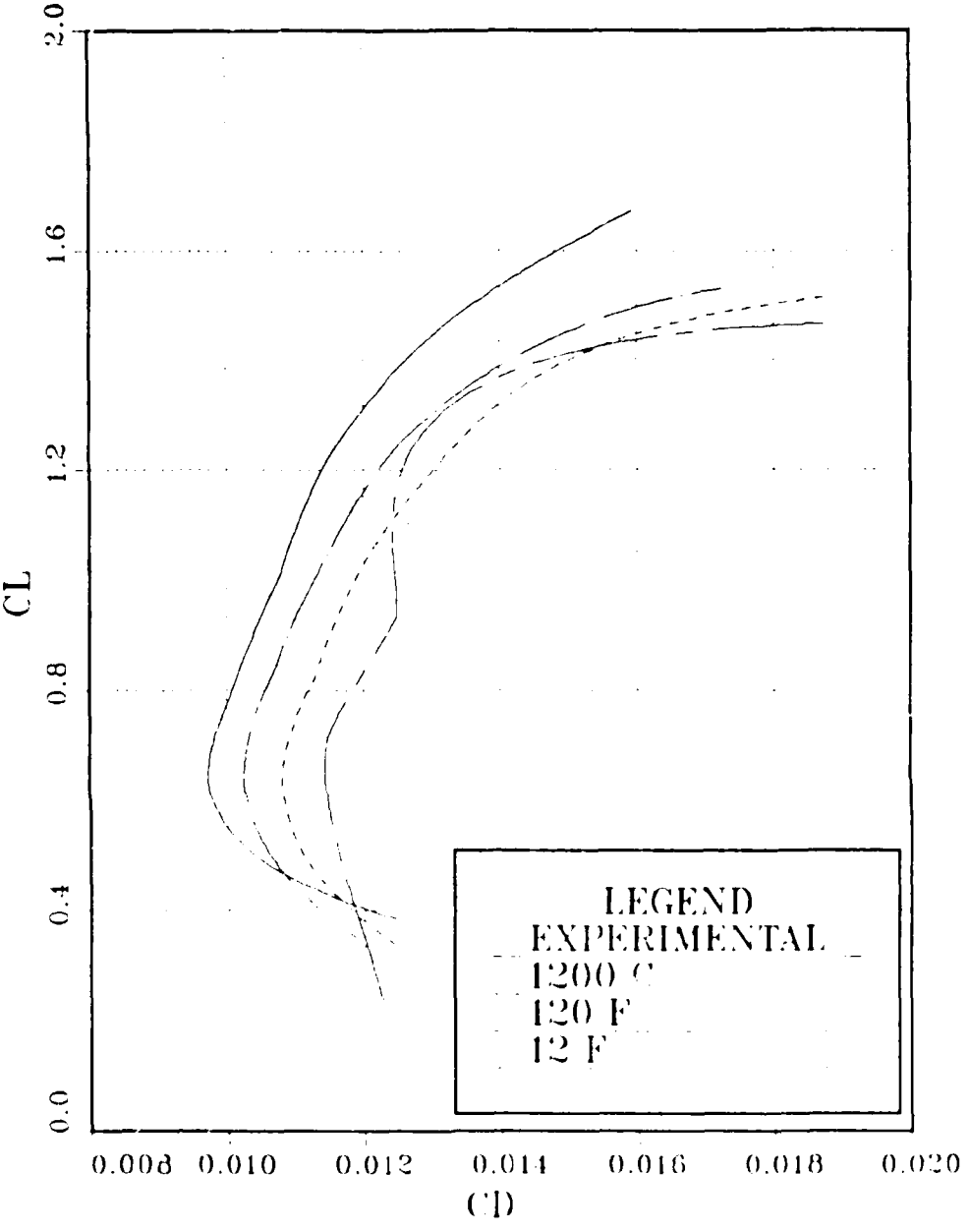

Figure 4.11 Comparison Of Drag Curves For Different Empirical Constants of γ_{tr} ($Re_{cr} = 0.28 \times 10^{6}$)

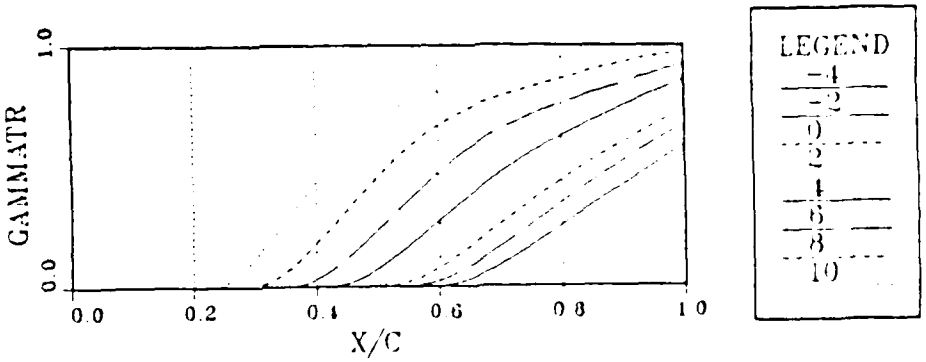

(a) $G_{\gamma_{tr}}$ = 1200

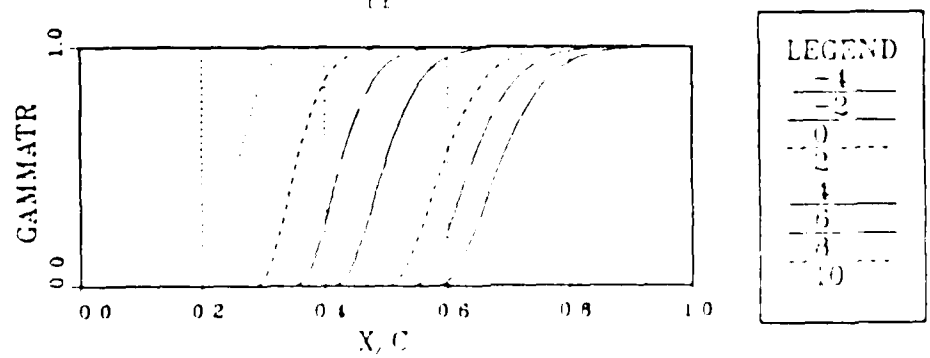

(b) $G_{\gamma_{tr}}$ = 12

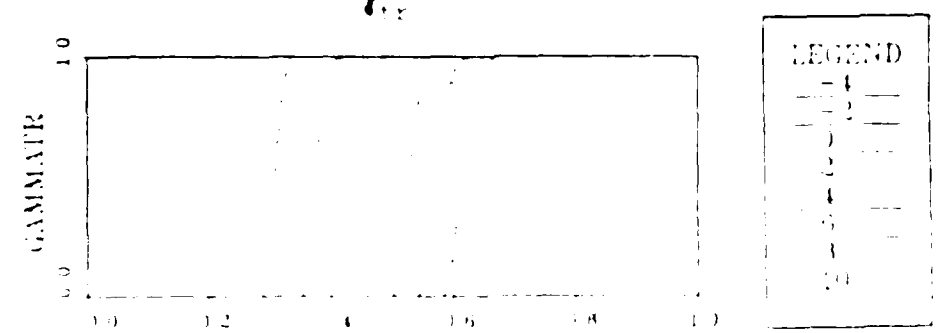

γ_{tr}

γ_{tr}

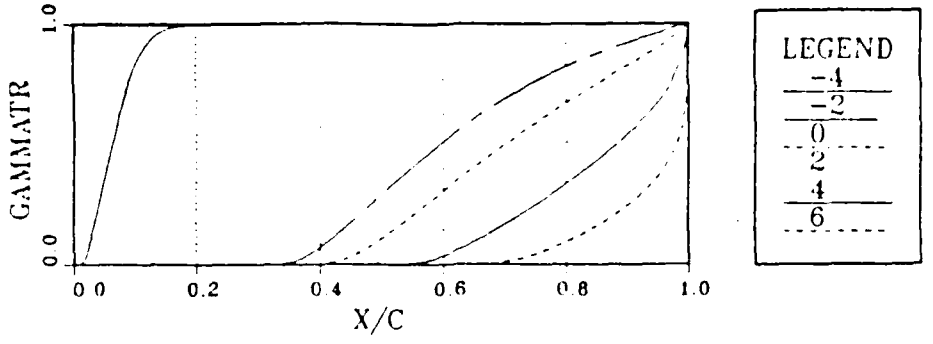

(a) $G_{\gamma_{tr}}$ = 1200

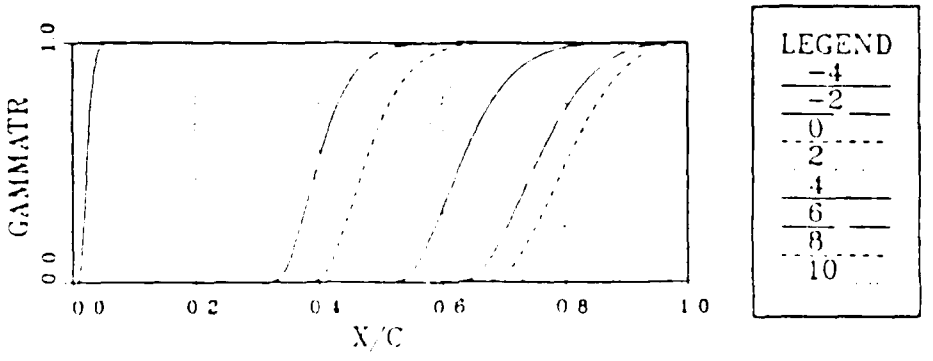

(b) $G_{\gamma_{tr}}$ = 120

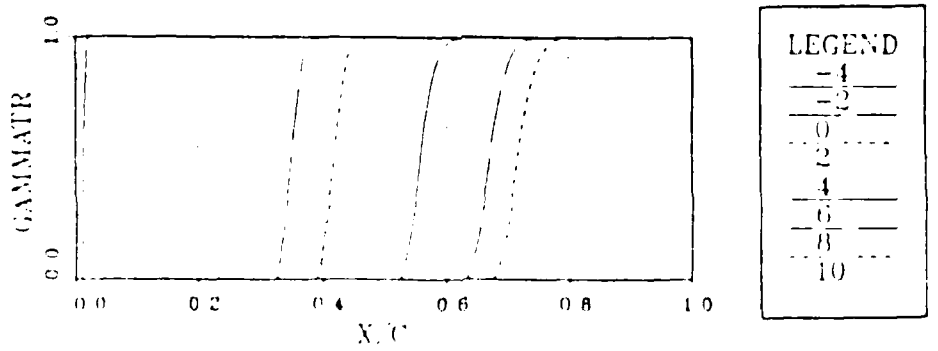

(c) $G_{\gamma_{tr}}$ = 1.

Figure 4.19 Comparison of Transition Length for Different Critical Coefficient $G_{\gamma_{tr}}$ At Lower Surface ($Re_{\infty} = \ldots \times 10^6$)

V. CONCLUSIONS

Cebeci's interactive computer program was applied to the Wortmann-Althaus FX 63-137 airfoil to show the capability of strong viscous/inviscid interaction methods to predict airfoil flows at low Reynolds numbers.

From the comparisons with the experimental data, it was confirmed that the results are closer to the experimental data as the Reynolds number increases.

Also, much better results were obtained by decreasing the empirical constant $G_{\gamma_{tr}}$.

Therefore, it was concluded that the boundary layer transition model has an important influence on the predictive capability of viscous/inviscid interaction methods.

LIST OF REFERENCES

1. Tuncer Cebeci and Peter Bradshaw, Momentum Transfer In Boundary Layers, McGraw-Hill Book Company, 1977.

2. Schlichting, H., Boundary-Layer Theory, McGraw-Hill Book Company, New York, 1968.

3. Peter Bradshaw, Tuncer Cebeci and James H. Whitelaw, Engineering Calculation Methods For Turbulent Flow, Academic Press, 1981.

4. Jack Moran, An Introduction to Theoretical and Computational Aerodynamics, John Wiley and Sons, 1984.

5. Paul K. Chang, Separation of Flow, Pergammon Press, New York, 1961.

6. Goldstein, S., On Laminar Boundary Layer Flow Near a Position of Separation, The quarterly Journal of Mechanics and Applied Mathematics, Vol. 1, 1948.

7. Abbott, I.H. and Von Doenhoff, A.E., Theory of Wing Sections, Dover, 1959.

8. Lighthill, M.J, On Displacement Thickness, Journal of Fluid Mechanics, Vol 4, 1958.

9. Althaus/Wortmann, Stuttgarter Profilkatalog I, Vieweg, 1979.

10. Arnold M. Kuethe and Chuen-Yen Chow, Foundations of Aerodynamics, Wiley, 1976.

INITIAL DISTRIBUTION LIST

		No. Copies
1.	Defense Technical Information Center Cameron Station Alexandria, Virginia 22304-6145	2
2.	Library, Code 0142 Naval Postgraduate School Monterey, California 93943-5002	2
3.	Chairman, Dept. of Aeronautics, Code 67 Naval Postgraduate School Monterey, California 93943-5000	10
4.	Personnel Management Office Air Force Headquarters Dae-Bang Dong Dong-Jak Ku Seoul, Korea	2
5.	Paik, Seung Woock 982-1, Sin-Jung 4 Dong Kang-Seo Ku (150-02) Seoul, Korea	10
6.	P.H. Subroto SMC 2735 Naval Postgraduate School Monterey, California 93943-5000	1
7.	Kim, Ju Eon SMC 1953 Naval Postgraduate School Monterey, California 93943-5000	2

END

4-87

DTIC